# **ENVIRONMENTAL RESEARCH**

# **LETTERS**

**TOPICAL REVIEW • OPEN ACCESS** 

How do intermittency and simultaneous processes obfuscate the Arctic influence on midlatitude winter extreme weather events?

To cite this article: J E Overland et al 2021 Environ. Res. Lett. 16 043002

View the <u>article online</u> for updates and enhancements.

### ENVIRONMENTAL RESEARCH

LETTERS



#### **OPEN ACCESS**

#### RECEIVED

16 September 2020

#### REVISED

30 December 2020

# ACCEPTED FOR PUBLICATION

13 January 2021

18 March 2021

Original content from this work may be used under the terms of the Attribution 4.0 licence.

Any further distribution of this work must maintain attribution to the author(s) and the title of the work, journal citation and DOI.



#### **TOPICAL REVIEW**

# How do intermittency and simultaneous processes obfuscate the Arctic influence on midlatitude winter extreme weather events?

J E Overland¹, T J Ballinger², J Cohen³,12, J A Francis⁴, E Hanna⁵, R Jaiser⁴, B -M Kim², S-J Kim<sup>8</sup>, J Ukita<sup>9</sup>, T Vihma<sup>10</sup>, M Wang<sup>1,11</sup> and X Zhang<sup>2</sup>

- NOAA/Pacific Marine Environmental Laboratory, Seattle, WA, United States of America
- International Arctic Research Center and Department of Atmospheric Science, University of Alaska Fairbanks, Fairbanks, AK, United
- Atmospheric and Environmental Research, Inc., Lexington, MA, United States of America
- Woodwell Climate Research Center, Falmouth, MA, United States of America
- School of Geography and Lincoln Centre for Water and Planetary Health, University of Lincoln, Lincoln, United Kingdom
- Atmospheric Physics, Alfred-Wegener-Institut, Helmholtz Centre for Polar and Marine Research, Potsdam, Germany
- Pukyong National University, Busan, Republic of Korea
- Korea Polar Research Institute, Incheon, Republic of Korea
- Niigata University, Niigata, Japan
- Finnish Meteorological Institute, Helsinki, Finland
- 11 The Cooperative Institute for Climate, Ocean, and Ecosystem Studies, University of Washington, Seattle, WA, United States of America
- Department of Civil and Environmental Engineering, MIT, Cambridge, MA, United States of America

Keywords: Arctic, jet stream, polar vortex, climate change, extreme weather, sea ice, Arctic amplification

#### Abstract

Pronounced changes in the Arctic environment add a new potential driver of anomalous weather patterns in midlatitudes that affect billions of people. Recent studies of these Arctic/midlatitude weather linkages, however, state inconsistent conclusions. A source of uncertainty arises from the chaotic nature of the atmosphere. Thermodynamic forcing by a rapidly warming Arctic contributes to weather events through changing surface heat fluxes and large-scale temperature and pressure gradients. But internal shifts in atmospheric dynamics—the variability of the location, strength, and character of the jet stream, blocking, and stratospheric polar vortex (SPV)—obscure the direct causes and effects. It is important to understand these associated processes to differentiate Arctic-forced variability from natural variability. For example in early winter, reduced Barents/Kara Seas sea-ice coverage may reinforce existing atmospheric teleconnections between the North Atlantic/Arctic and central Asia, and affect downstream weather in East Asia. Reduced sea ice in the Chukchi Sea can amplify atmospheric ridging of high pressure near Alaska, influencing downstream weather across North America. In late winter southward displacement of the SPV, coupled to the troposphere, leads to weather extremes in Eurasia and North America. Combined tropical and sea ice conditions can modulate the variability of the SPV. Observational evidence for Arctic/midlatitude weather linkages continues to accumulate, along with understanding of connections with pre-existing climate states. Relative to natural atmospheric variability, sea-ice loss alone has played a secondary role in Arctic/midlatitude weather linkages; the full influence of Arctic amplification remains uncertain.

### 1. Introduction

If and how recent Arctic changes influence broader hemispheric weather continues to be an active and controversial research topic [1-6]; e.g. Cohen et al [5] noted 146 papers on the subject. It remains a significant research challenge and a potential opportunity to improve extended-range forecasts,

as noted by the recent Year of Polar Prediction project [7]. Understanding the potential influence of disproportionate Arctic warming on frequency and persistence of extreme winter weather events in midlatitudes is societally relevant, as continued Arctic amplification (AA) of temperature increase is an inevitable aspect of anthropogenically forced global change (e.g. [8, 9]). Severe and aberrant winter weather has major impacts on infrastructure, transportation, agriculture, productivity, recreation, public health, and ecosystems. The influence of Arctic change on global weather patterns is already motivating efforts to mitigate climate change [10].

Reviews [5, 11] and international workshops, sponsored by the World Climate Research Programme's Climate & Cryosphere project, International Arctic Science Committee (IASC), and the U.S. Climate Variability and Predictability program, reached divergent conclusions on the relative importance in Arctic/midlatitude linkages between AAforced changes and atmospheric internal variability, based on model simulations and observational data. While many recent studies have identified associations and mechanisms linking sea-ice loss and/or AA with various winter extreme weather regimes in midlatitudes (e.g. [5, 12], and references therein), some conclude that thermodynamic forcing due to recently sea-ice-free Arctic regions is insignificant relative to internal atmospheric variability [2, 6, 12-21]. Several implicate a particular dominance of an upstream teleconnection forcing from the Atlantic that amplifies warming over the Barents/Kara Sea (BK) region, regional ridging of high pressure systems, and then downstream cooling over Asia [22-26]. A subset of these investigations focuses on warm air advection into the BK region [23, 27]. Other forcings include local heating of the atmosphere, not necessarily from the loss of sea ice [12, 28], and tropical influences [29–31]. A large number of papers (27 [5]) based on climate model simulations do not support sea-ice loss as a significant mechanism for Arctic/midlatitude weather linkages. Recent work suggests that models can underestimate the atmospheric response to AA [12, 32-34]. Potential Arctic influences remain unresolved, but it is generally accepted that possible Arctic/midlatitude weather linkages are not always direct, can be overwhelmed by internal variability, and are often subject to multiple, simultaneous, and timelagged ocean-atmosphere processes.

An advance in understanding high-latitude climate change is that Arctic/midlatitude weather linkages depend not only on the magnitude of AA, but also on the location, amplitude, and movement of meanders in the polar jet stream [22, 35–37]. That this connection does not appear in all years or all months is an argument for the intermittency of weather linkages despite continued AA. Spatial and temporal variations in AA patterns also contribute to intermittency [38]. Inspection of year-to-year variability reported in studies claiming weak multi-decadal trends in linkages (e.g. [39]), suggests such intermittency. In fact, amplified Arctic warming may not initiate midlatitude connections, but instead intensify intrinsic linkages by enhancing the amplitude of existing large-scale Rossby waves—subject to the influences of sea-surface temperature (SST) anomaly patterns and geographic features—and therefore contribute to the formation of stationary blocking anticyclones [37, 40]. Amplified Rossby waves lead to increased northward warm advection as well as southward cold advection between the subarctic and midlatitudes. Some metrics of jet-stream waviness (e.g. sinuosity, meridional circulation index, local wave activity flux) have indicated an increased frequency of high-amplitude jet stream days since AA emerged in the mid-1990s, embedded within large year-to-year winter natural variability [41-46]. Because cold and warm extreme events often occur simultaneously in adjacent regions, according to the axis and amplitude of jet-stream waves as they progress, metrics based on averages over a season, across large regions, or over many model ensemble members tend to produce insignificant composite signals [3, 47]. This fact is one source of discrepancy among studies.

Three Arctic processes are potentially involved in feeding back to dynamic longwave atmospheric patterns: (a) local thermodynamic surface forcing, often associated with loss of sea ice; (b) northward warm air advection into an existing longwave ridge; and (c) internal atmospheric blocking processes that add to the persistence of the wavy jet stream pattern. The state and balance of these three regional factors comes from a qualitative interpretation of the geopotential height tendency equation in pressure coordinates (from [48], which is a modified version of equation (6.14) from [49]):

$$\chi \propto f_0 \mathbf{V}_g \cdot \nabla \left( \frac{1}{f_0} \nabla^2 \Phi + f \right) + \frac{f_0^2}{\sigma} \frac{\partial}{\partial p} \left[ \mathbf{V}_g \cdot \nabla \left( \frac{\partial \Phi}{\partial p} \right) \right] + \frac{f_0^2 R_d}{\sigma c_p} \frac{\partial}{\partial p} \left( \frac{dQ/dt}{p} \right)$$
(A)
(B)
(C)

where  $\chi = \partial \Phi / \partial t$  is defined as the geopotential tendency, and the static-stability parameter  $\sigma$  is defined as  $\sigma = -(\alpha/\theta)(\partial \theta / \partial p)$ ,  $\theta$  is potential temperature,  $\alpha$  is specific volume,  $\Phi$  denotes the geopotential height,

 $f(f_0)$  is the Coriolis parameter (at 45°),  $\mathbf{V}_g$  is the geostrophic wind,  $R_d$  is the gas constant for dry air,  $c_p$  is the specific heat at constant pressure, and Q is the external heating. Geopotential heights rise and fall proportional to negative and positive absolute

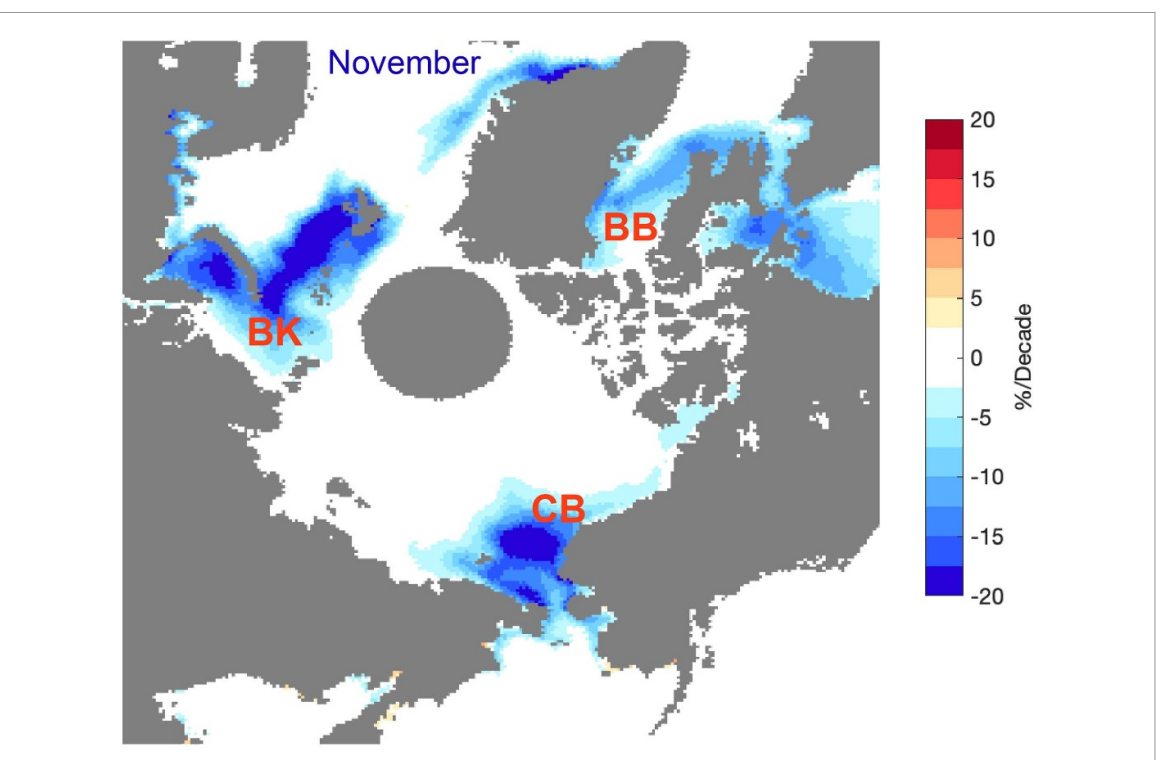


**Figure 1.** Linear trend of November sea-ice concentration (SIC) in the period 1979–2019. This pattern highlights the delay of sea-ice freeze-up in the Barents/Kara Seas (BK), Chukchi/Beaufort Seas (CB), and Baffin Bay (BB). SIC data are obtained from the National Snow and Ice Data Center (NSIDC), https://nsidc.org/data.

vorticity advection (Term A), vertical variation of geopotential thickness (heat) advection (Term B), and low-level diabatic heating (Term C). Authors discussing Arctic/midlatitude connections often focus on the third element, ocean-to-atmosphere heat flux owing to the loss of sea ice associated with AA, but the first two factors are important in midlatitude linkages. Tying midlatitude weather regimes to internal atmospheric variability of the regional jet stream, which can be modulated by Arctic forcing, provides physical insight into linkage theory.

The delay of fall freeze-up of sea ice is one of the most conspicuous manifestations of the changing Arctic. It occurs regionally with the largest changes in BK, Baffin Bay (BB), and the Chukchi/Beaufort Seas (CB) (figure 1). Owing to increased turbulent and radiative fluxes from the surface to the atmosphere in ice-free Arctic areas during early winter, one would expect some direct tropospheric geopotential thickness increases in these regions through at least January, the typical time when freeze-up tends to be complete across the Arctic Ocean and its marginal seas. Two studies that link surface turbulent fluxes to atmospheric circulation are [50] and [51].

During late winter when the Arctic Ocean is generally frozen over, Arctic/midlatitude connections are generally less attributable to direct ocean-atmosphere heat fluxes related to sea-ice loss, although as the ice thins, heat fluxes increase in influence. A major controlling factor for classic late-winter cold-air outbreaks into midlatitudes is the linkage to the

occurrence of stratospheric polar vortex (SPV) disruptions and displacements over the continents. Accordingly, improved understanding of factors causing SPV disruptions is required. A cluster analysis of daily, pan-Arctic 100 hPa geopotential height anomalies derived from ERA-Interim Reanalysis during January/February 1979-2018 suggests five dominant circulation patterns (figure 2, from [52]). Cluster 1 is a pole-centered region of lower-thanaverage 100 hPa heights that represents a strong SPV. The corresponding time series indicates a decrease in the seasonal-mean frequency of this pattern since 2000. Other clusters represent progressively weaker states of the SPV, in terms of mean polar-cap geopotential heights. Cluster 5 exhibits a positive height anomaly centered over Greenland/central Arctic, indicative of a weak SPV related to sudden stratospheric warmings (SSWs). Clusters 2 and 4 represent an SPV center shifted southward over North America and west of Greenland and occur in more than 40% of the record. As discussed by [52], configurations classified as cluster 5 were more frequent during the last decade, while clusters 2 and 4 occurred relatively frequently during the last 5 years of the analysis (figure 2).

This review focuses on the differences between early- and late-winter processes involved in Arctic/midlatitude linkages and acknowledges that not all Arctic/midlatitude weather connections necessarily originate from recent AA. We consider open science questions, address recent studies, and note the

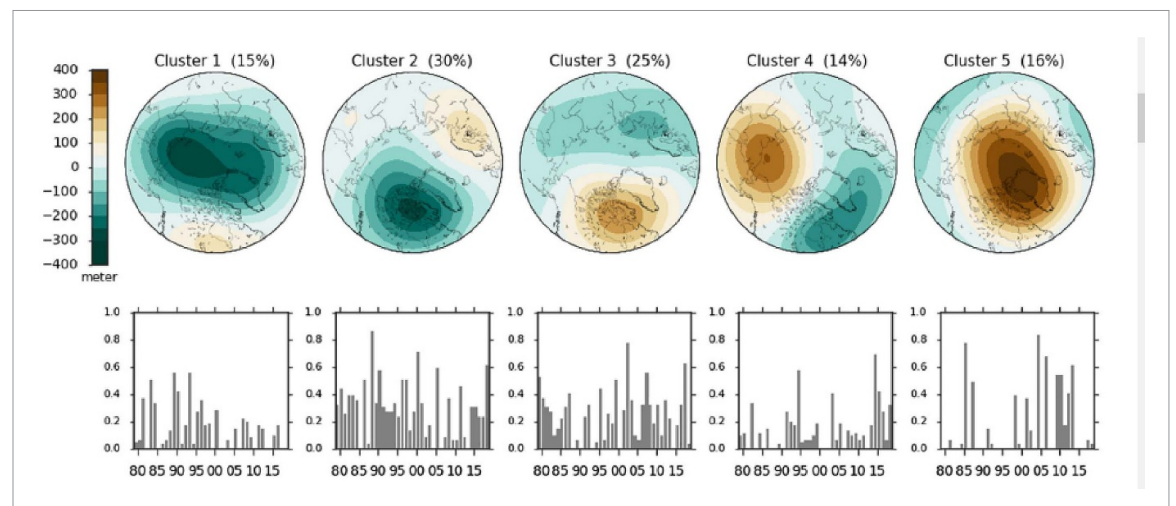


Figure 2. Representative clusters of 100 hPa geopotential height anomalies (m) during winter (JF) from 1979 to 2018. Numbers in parentheses above each map reflect the percentage of occurrence. Bar plots present seasonal-mean normalized frequency of occurrence during each year. Reprinted from [52]. Copyright © 2018, The Author(s). CC BY 4.0.

interaction of multiple processes that have received less attention in the literature. We organize the review geographically as follows: (a) East Asian weather connections to BK sea-ice loss, (b) North American weather events and their relationship with early-winter ridging and late-winter SPV disruptions, (c) European severe weather, and (d) possible SPV modulations based on tropical connections.

# 2. Linkages affecting Asia

Since the beginning of the 21st century, cold spells over East Asia occurred not only more frequently, but they were stronger and more persistent than during previous decades [53-55]. In December 2009, 2012; January 2008, 2010, 2013, 2016; and February 2008, 2018, bitter cold periods and heavy snowfall accompanied by freezing rain in some areas struck East Asia, resulting in severe economic and societal disruption [56, 57]. Previous studies based on statistical analyses of reanalysis data, as well as sensitivity experiments using both atmosphere-only and atmosphereocean coupled models, provided evidence supporting a relationship between negative surface air temperature (SAT) anomalies over East Asia and lower-thanaverage sea-ice extent in the central Arctic Ocean and/or the BK [11, 32, 35, 39, 58-62]. Recent cooling in Central Asia accompanied by Arctic warming is called warm Arctic/cold Eurasia (WACE) pattern [32, 60, 63]. According to the WACE index, the positive WACE coincides with an anomalously low BK sea-ice cover with a correlation coefficient of -0.52 at 99% confidence level (figure 3). The connections between WACE and BK sea-ice cover can be a consequence of an interactive process mediated by a changing atmospheric circulation [64], in which the BK sea-ice anomaly is a response to regional internal variability and/or BK can force the atmospheric circulation [63].

Further, the same atmospheric circulation that results in a cold Eurasian continent also directly contributes to BK sea ice loss, as Ural blocking results in advection of southerly air masses over the BK [65].

Two main pathways, a tropospheric pathway and a stratospheric pathway, have been proposed that provide plausible explanations for the statistical relationships between Arctic change and midlatitude weather [11]. Numerous observational and modeling studies relate BK sea-ice co-variability to winter midlatitude circulation patterns in both the troposphere and stratosphere; some studies find no robust connection (see [5, 66, 67] for comprehensive reviews).

# 2.1. Early-winter tropospheric processes

The tropospheric pathway is pronounced in November to December and is discussed in conjunction with a stationary Rossby wave train excited by anomalous diabatic surface forcing, partly from sea-ice loss in the BK region (e.g. [5, 59], and references therein). When looking at a broader spatial area, a wave train originating in the northern North Atlantic Ocean and extending to Eurasia is common, in part associated with positive SST anomalies along the eastern seaboard of North America [23] and extending eastward to the Ural Mountains (figure 4, far left).

A description of the dominant atmospheric circulation patterns over the extended winter season under low (2001/2002–2013/2014) and high (1978/1979–1999/2000) Arctic sea-ice conditions was provided in [68]. In early winter, an anticyclonic pattern over Scandinavia that extends toward Siberia, referred to as the positive phase of the Scandinavian pattern (SCAN), occurs significantly more often under low Arctic sea-ice conditions (figure 5, tall red bars for SCAN). During SCAN blocking episodes the crests of planetary waves extend into the Arctic causing high baroclinicity; northward ocean advection into

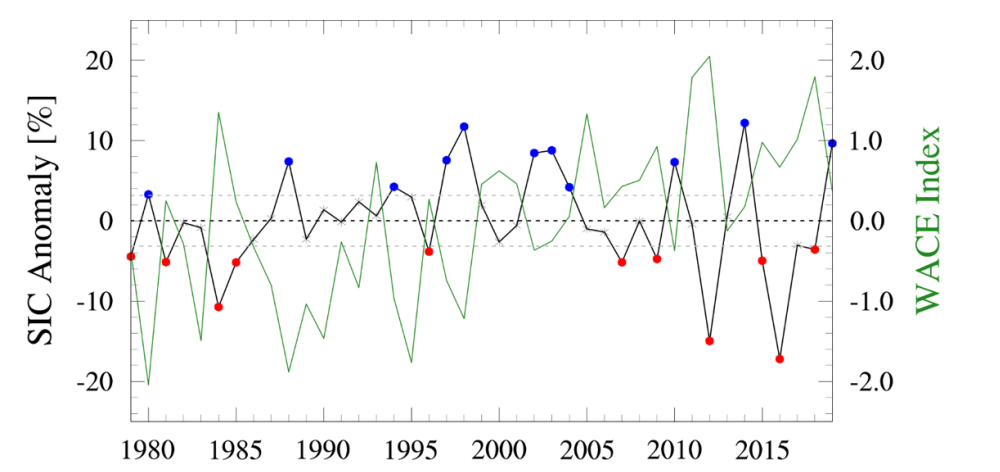


**Figure 3.** Time variation of the mean sea-ice concentration anomaly over the BK (black) and WACE index (green) in early winter (November and December). Blue (red) dots represent the years when the sea-ice cover was more than 0.5 standard deviation (gray dashed lines) above (below) the mean during 1979–2019 (black dashed line). Sea-ice concentration data are from HadISST (www.metoffice.gov.uk/hadobs/hadisst/), and the WACE index is estimated as the difference in surface air temperature between the BK (65° N–82° N, 10° E–100° E) and central Asia (40° N–60° N, 70° E–120° E) using the NCEP-DOE Reanalysis 2 data (https://psl.noaa.gov/data/gridded/data.ncep.reanalysis2.html).

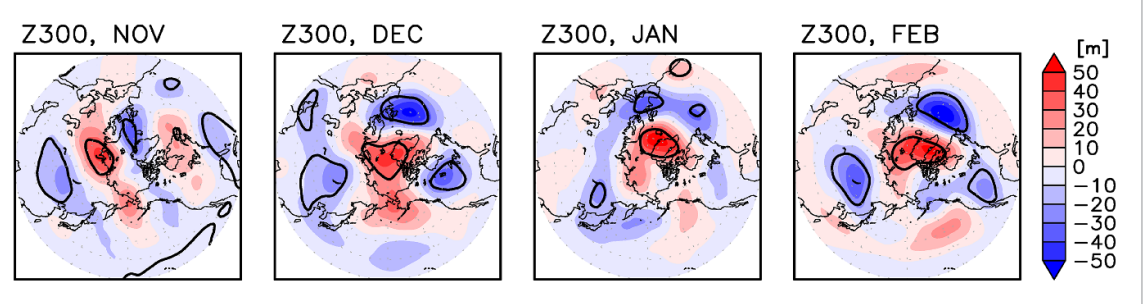


**Figure 4.** Regression maps of monthly averaged geopotential heights at 300 hPa from November to February for winters from 1978/79 to 2014/15, regressed onto the detrended and normalized November-averaged BK (70–85° N, 15–90° E) SIC index. The sign of the coefficients is reversed, such that positive (negative) height anomalies are associated with negative (positive) SIC anomalies. Heavy black contours indicate where statistical significance exceeds the 95% level. The analysis is based on geopotential heights from the Japan Meteorological Agency JRA-55 reanalysis (www.jra.kishou.go.jp/JRA-55/) and the Met Office Hadley Centre HadISST2 sea ice data (www.metoffice.gov.uk/hadobs/hadisst2/).

the Barents Sea should add to loss of sea ice as a forcing [69]. The appearance of the SCAN pattern often coincides with the occurrence of the North Atlantic-BK-Asia wave train [70–72]. Lack of BK sea ice and extensive autumn snowfall anomalies over Siberia are not necessarily causes for the atmospheric wave train across Eurasia but may contribute to the initiation and reinforcement of a Ural blocking pattern [23, 60], which can further reduce the BK sea-ice cover [70]. In early winter all three mechanisms (equation (1)) are involved: surface heat flux, warm-air advection, and blocking.

On seasonal timescales, blocking in the Ural region can establish a cold reservoir in central Siberia, which can affect subsequent downstream synoptic weather events that advect cold air-masses into eastern Asia. The figure 6 composite of winter anomaly maps from 1979 to 2019 captures synoptic conditions during November–March over Eurasia prior to the onset of cold surge events in East Asia,

when the BK sea-ice cover was more than 0.5 standard deviations below the climatological mean during early winter (November and December) (figure 3). The onset and termination of the cold event are defined when daily mean SAT over East Asia (35°-45° N;  $120^{\circ}-130^{\circ}$  E) exceeded -1.5 standard deviations over 2 d (onset), then the daily mean SAT recovered to the climatological mean (termination). From day −6 to day 0, the area of anomalously low SATs relative to the climatological mean, high sea-level pressure (SLP), and geopotential height at 300 hPa all moved southeastward from the BK and Ural Mountains to East Asia. The negative SAT anomaly occurred due to cold advection from the expansion of the high geopotential height anomaly [59, 73, 74]. From days -6to 0, an upper-level atmospheric wave pattern consisted of negative geopotential height anomalies over northern Europe and Lake Baikal and its surroundings, and positive height anomalies over the BK and the Ural Mountains. A strong east-west SLP gradient

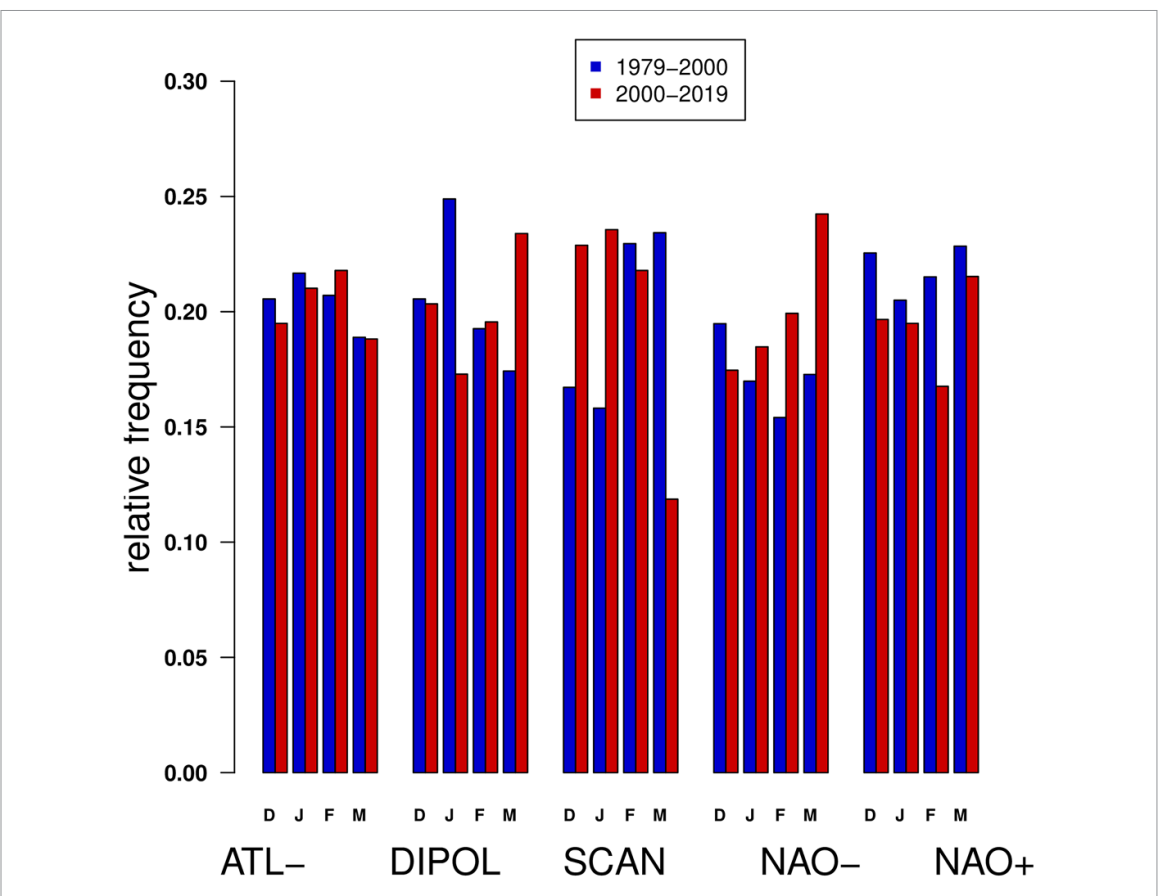


Figure 5. Relative frequency of five large-scale atmospheric patterns during December, January, February, and March 1979–2019 with respect to Arctic sea-ice conditions from ERA-Interim. Blue bars represent the relative frequency of occurrence for high ice conditions, and red bars for low ice conditions. The five patterns, resolved through cluster analysis on sea-level pressure fields, are identified as North Atlantic Oscillation (NAO+), SCAN, ATL-, NAO-, and dipole (reprinted from [68]. ©2017 The Authors. Published by Elsevier B.V. CC BY 4.0.). Note the frequent occurrence of the SCAN pattern in early winter and the NAO- pattern in later winter for low sea ice conditions.

formed (figure 6(i)), promoting northerly winds and cold surges across East Asia (figure 6(c)).

A record event occurred in late December 2020 representing a classic Ural High and a deep coastal Asia/North Pacific low, with a 1094 hPa high, 920 hPa low, and a major eastern Asia cold event.

#### 2.2. Late winter pathway

The second mechanism, termed the stratospheric pathway, has a longer timescale extending from mid- to late-winter (e.g. [5, 11, 58, 61, 75, 76]). It is characterized by a series of dynamically consistent, time-lagged relationships, i.e. enhanced vertical propagation of planetary-scale Rossby waves that weaken the SPV, followed by a downward progression of connections to the troposphere and a resultant negative North Atlantic/Arctic Oscillation (NAO/AO) in January through March (figure 4, right) [58, 77–80]. Observational studies link the recent increase in weak SPV events (cluster 5 pattern in figure 2) to negative sea-ice anomalies in the BK (figure 3), and negative NAO in February and March (figure 5) [58]. However, modeling studies provide only mixed support for these relationships, although some models

with a well resolved stratosphere and/or interactive stratospheric chemistry more realistically simulate observed linkages between BK sea-ice loss and a weakened SPV [5, 81].

During late winter, a circulation pattern similar to the negative phase of the NAO is preferred when low-ice conditions occur, indicated by the taller red bars than blue bars in February and March for NAO – in figure 5. A negative NAO is the most common response following weak SPV events along with the corresponding downward propagation of positive polar cap geopotential height anomalies from the stratosphere to the surface [61, 82, 83]. The time-lag regression of February 300 hPa geopotential height anomalies on the November BK sea ice anomaly (farright of figure 4) provides supporting evidence for a NAO shift toward the negative phase in late winter, with a high/low dipole of anomalous heights over the Nordic Seas and the North Atlantic. Anomalously extensive snow cover and cold soil temperatures during fall can influence winter weather in Asia by preconditioning (albedo and temperature) and through positive feedbacks [84-87], although some studies question these interactions (e.g. [70, 75]).

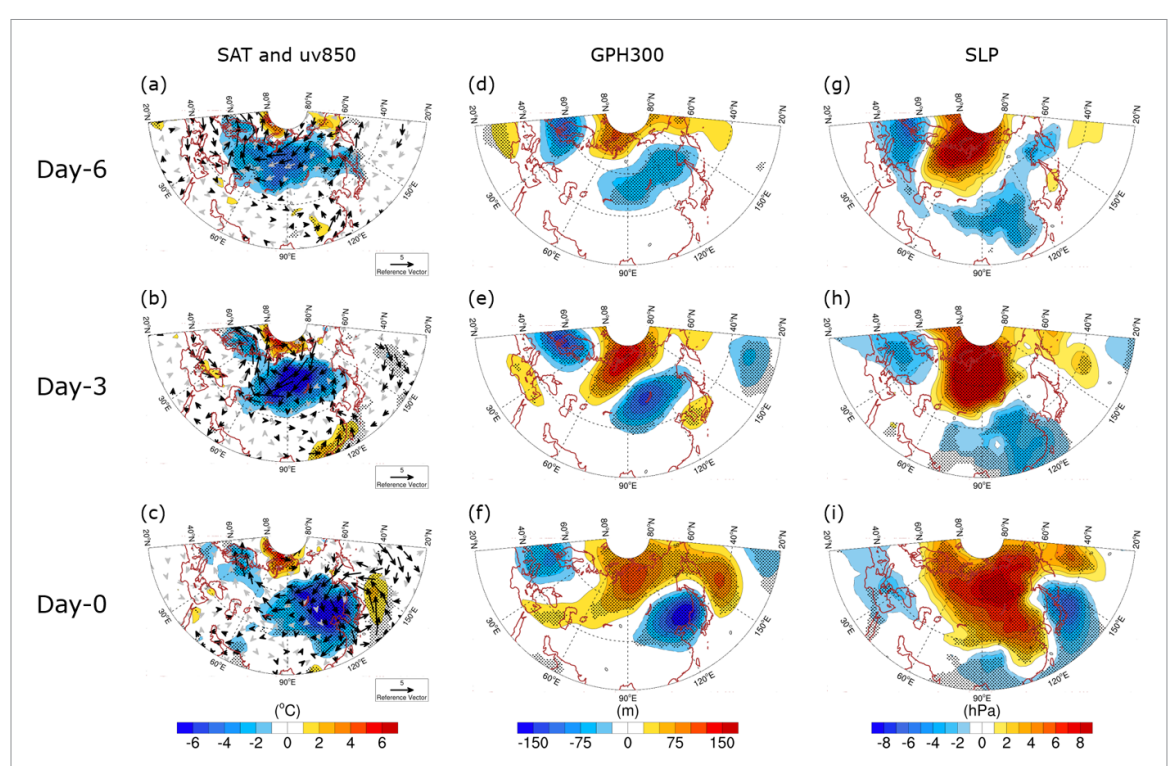


**Figure 6.** Composite anomaly maps of winter (November through March from 1979 to 2019) for (left) surface air temperature (SAT,  $^{\circ}$ C) with wind vectors (m s $^{-1}$ ) at 850 hPa, (middle) 300 hPa geopotential height anomalies (m), and (right) sea-level pressure anomalies (hPa), when the BK sea-ice concentration is at least 0.5 standard deviation lower than normal in early winter (November and December), as shown in figure 3. Top to bottom: 6 d before, 3 d before, and the day of cold-surge occurrence. Wind vectors and SAT, 300 hPa geopotential height anomalies, and sea level pressure anomalies significant at 95% confidence level are represented as dark arrows and dots, respectively, from student's t-test. Data are from NCEP/NCAR reanalysis.

Challenges remain in understanding how the wave train over the North Atlantic-Eurasian sector and the phase shift to the negative NAO evolve over the extended winter season (November to March). Table 1 summarizes the potential impacts of BK seaice loss on weather in Asia during early- versus latewinter. Despite evidence of Arctic/midlatitude linkages during some SSW events, not all such episodes result in strong troposphere cooling, as was the case with the marked SPV weakening of February/March 2019 [88].

# 2.3. A case study for the impacts of local heat fluxes

Here we use a recent case study to better understand underlying physical mechanisms between BK sea-ice/SAT and atmospheric conditions over Asia, augmenting previous discussions based on statistical approaches. To demonstrate the usefulness of synoptic-scale analysis, we present potential vorticity (PV) fields and a daily evolution of anomalies in SAT, turbulent heat fluxes, sea-ice concentrations (SICs), and downward longwave radiation fluxes (DLR) for the remarkable amplification of the Arctic warm anomaly that occurred in late December 2015 to early January 2016 [65, 89, 90] followed by an exceptional cold spell in East Asia during late January.

According to the operational analysis from the European Centre for Medium-Range Weather

Forecasts, high Arctic SAT exceeded 0 °C in early January 2016, a value 25 °C above the winter climatological mean with a record high daily temperature since 1950 [91]. Following this warm event, a large reduction in the Arctic sea-ice extent occurred in the middle of the cold season [92–95], and a cold wave struck much of East Asia in late January 2016, bringing record low SATs and snowfall to many parts of southeast and central Asia [90, 96, 97].

Figure 7 presents daily isentropic PV fields for 28-31 December 2015, when an abrupt temperature increase began over the BK. On 28 December 2015, a lobe of low PV (less than 5 PV units on the 330 K isentropic surface, approximately 300 hPa) intruded into the Arctic with a corresponding warm air flow into the Arctic (figure 7(a)). At the same time, an area of high PV developed and amplified to the south on both sides of the low PV over the North Atlantic. During 29–31 December 2015, the low PV region reached its minimum value over the BK (figures 7(b)-(d)). The warm and humid air intrusion from lower latitudes reached the central Arctic, showing an active role in the initiation of the extreme warming event. The high PV to the south developed to its maximum value and a gradual reversal of the PV gradient occurred, indicating a cyclonic wave-breaking event, which is a typical initial indicator of block formation. A precursor to the warm BK event was thus

**Table 1.** Summary of sea-ice related anomalies from the lagged-regression analysis using the detrended November-averaged Barents-Kara (30–90° E and 65–85° N) sea-ice concentration time series, such as in figure 4 for 300 hPa geopotential height data. Supporting information: \*: results are similar to figure 2 but using an analysis based on monthly averaged sea level pressure (SLP) and surface air temperature (T-2m) fields. \*\*: similar to figure 4 but the analysis is based on the daily zonal-mean zonal winds at 60° N and the vertical Eliassen-Palm flux (i.e. EP-flux) component averaged over 40–80° N at 100 hPa. The analyses are for the winters from 1979/80–2016/17. The features listed are also discussed by [5, 58, 59, 61, 80].

	Early winter		La	Late winter	
	Nov	Dec	Jan	Feb	Ref. and Notes
Tropospheric circulation • Wave train from North anomalies  Atlantic to Eurasia  • Deeper Icelandic Low in Nov		• NAO becomes more negative in Feb		Figures 6 and 7	
Surface conditions in Siberia	<ul><li>Siberian hi</li><li>Surface ten</li></ul>	*			
Stratospheric polar vortex (SPV)		•	Progressively	weaker	**
Vertical EP-flux component	Increase in D	lec	A large peak subsequent v		**

internal atmospheric variability from vorticity advection (Term A in equation (1)).

After the initiation of the abrupt warming by the intrusion of a low-PV airmass, a WACE pattern developed during the first 10 d of January 2016. Over the following 10 d, positive SAT anomalies over the BK decreased. During the evolution of this extreme event, a stationary positive geopotential height anomaly persisted for nearly a month over the Ural Mountains region, a Ural blocking event [74, 98, 99].

We examined the BK regional co-variability of daily SAT and sea ice anomalies (figure 8(a)), along with area-averaged turbulent heat fluxes and DLR during this event (figure 8(b)). Here, the BK region is defined by  $76^{\circ}$  N– $83^{\circ}$  N,  $20^{\circ}$  E– $80^{\circ}$  E. In figure 8(a), the local temperature variation leads SIC variation by 1 or 2 d. Note that SAT increases abruptly on 28-29 December 2015 (figure 8(a)), coincident with the PV analysis shown in figures 7(a) and (b), which indicates intrusion of a low-PV airmass to BK from lower latitudes [92]. The DLR anomaly in figure 8(b) is strongly correlated with the SAT anomaly in figure 8(a) (r = 0.92). On daily time scales, the anomalies in turbulent heat flux and SIC are not identifiably correlated. Nevertheless, the turbulent heat flux exhibits an anti-correlation with DLR on daily time scales (r = -0.69), with DLR slightly leading the turbulent heat flux. This suggests periods of warmer SAT and humid air flow, illustrating the active role of warm and moist air advection (Term B in equation (1) in driving both surface warming and sea-ice melt over the BK [22, 28, 100-102]. Assuming that a positive DLR anomaly is indicative of a warm-air intrusion, we note that the several events occurred with less than a 10 d life cycle (figure 8(b)). At the same time, the overall sea-ice cover of the BK during winter of 2015/16 was well below normal (figure 8(a)). In summary, integrating through the entire period from 20 December 2015 to 10 February 2016, the turbulent heat flux anomaly is positive (upward), contributing to amplified Arctic warming

due to sea-ice loss, while warm-air advection is episodic (figure 8(b)).

#### 3. North America

#### 3.1. Early winter tropospheric pathway

Over North America in early winter, loss of sea ice in CB may reinforce an existing climatological ridge/trough jet stream pattern [36, 39, 51, 63, 103, 104], although it is clear that the connection does not occur in every year despite continuing AA. It is thus worthwhile to investigate year-to-year shifts in the background jet stream pattern. The pattern in December 2016 contrasts with December 2017 (figure 9). During both years, sea-ice freeze-up was delayed in association with abnormally warm SAT in the CB; in 2017 the anomalously warm SAT reinforced the climatological wavy jet stream over North America [51] and downstream trough with cold eastern U.S. temperatures [39, 63, 105] (figure 9(b)), while in 2016 (figure 9(a)) the more zonal prevailing jet stream was located too far south to tap into the surface heat source north of Alaska. During 2016 the northeast Pacific also featured a cold SST anomaly that stretched latitudinally along  $\sim 45^{\circ}$  N, which favored an enhancement of the southern located

To put December 2017 in context, figure 10 shows the time series of December cold and warm temperature events over the eastern U.S. and the indices of ridging (500 hPa geopotential heights) over Greenland/Baffin Bay (GBB) and Alaska ridging (AR). AR was associated with the 2017 pattern, GBB blocking was influential in 2010, and ridging in both regions was coincident with the eastern U.S. cold event in 2000. During warm Decembers, AR and/or GBB indices tend to be negative. Note that five major cold events in the 1980s occurred before the emergence of significant AA, dominated by internal atmospheric variability [51]. showed quantitatively

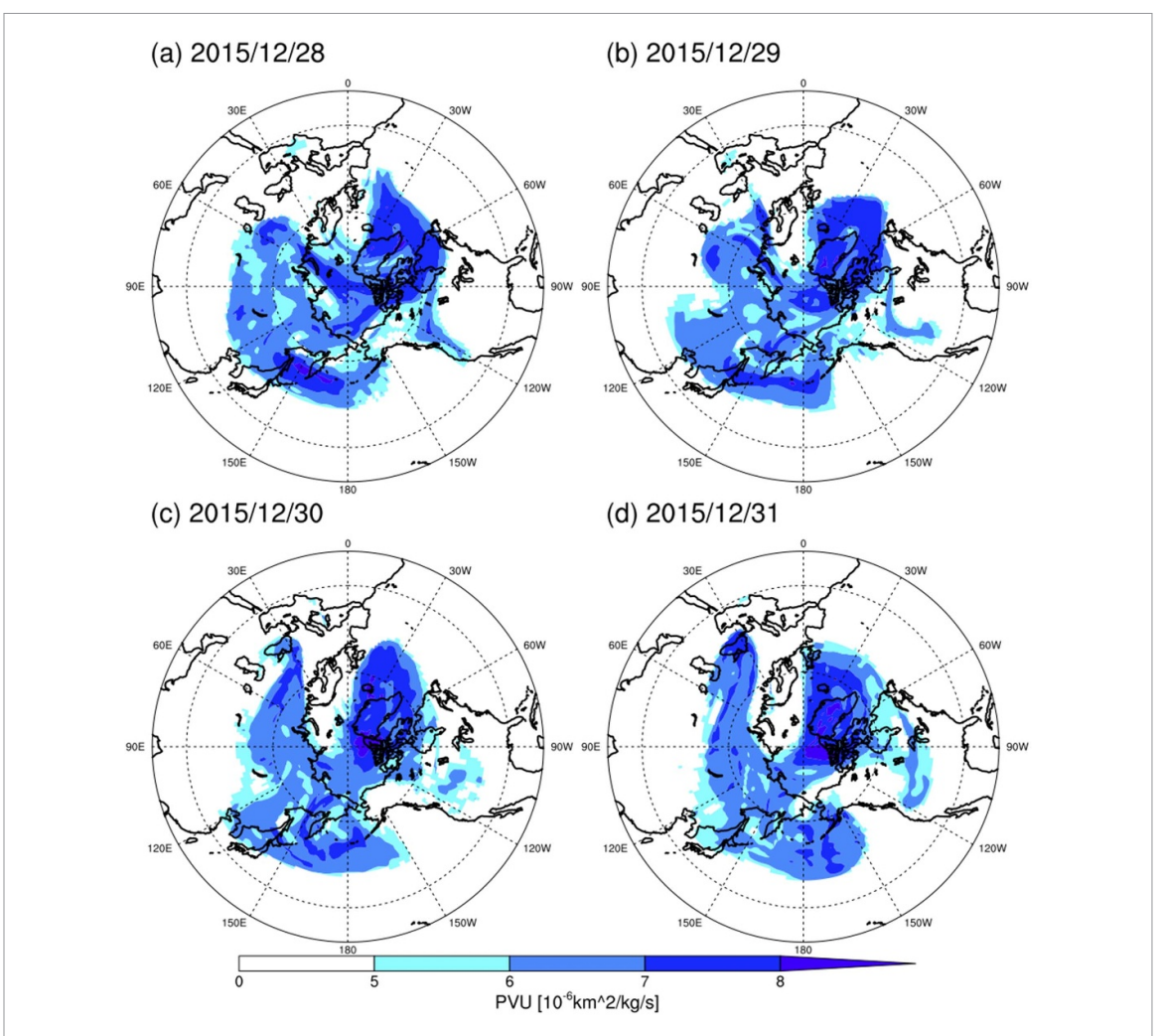


**Figure 7.** Evolution of daily-mean potential vorticity (PV) at 330 K in the Northern Hemisphere for the period of extreme Arctic amplification that occurred during late December 2015 (a)–(d). For better visualization, only areas with PV over 5 PV units (PVU) are shaded (1 PVU =  $10^{-6}$  km<sup>2</sup> kg<sup>-1</sup> s<sup>-1</sup>). Data are from the Japan Meteorological Agency JRA-55 reanalysis (www.jra.kishou.go.jp/JRA-55/).

that all three potential linkage mechanisms contributed to the North American weather pattern during early winter 2017 (equation (1)): direct ocean surface fluxes (their figure 6(b)), warm air advection, and a wavy background jet stream. A key implication from figure 10 is that the jet stream configuration was not favorable for an early-winter monthly weather linkage between the Arctic and North America in most recent years [106] with the notable example of extreme warmth in 2015 accompanied by negative AR and GBB. Also apparent is that wavy jet stream patterns were associated with cold winters in eastern North America before the start of AA due to the connection between an AR or GBB index and the cold temperature anomalies. Individual cold spells can span less than a month preceded or followed by warm anomalies, thus monthly averaging may obscure linkage events with durations on sub-monthly timescales.

While the direct connection with the fall-early winter jet stream is in December, an interesting new case is late October 2020 (figure 11). Figure 11(b) shows the jet across the eastern North Pacific well

south of the Arctic but with a slight ridge as seen in the height anomaly pattern due to warm near surface temperatures (figure 11(a)). Warm Arctic temperatures contribute to a separate height anomaly and ridging over Alaska (figure 11(b)). The combination of the North Pacific and Alaskan ridging supports the North American ridge/trough pattern with record October cold temperatures in the central plains of the U.S. and southern Canada.

#### 3.2. Late winter pathway

In late winter conditions leading to persistent cold spells in central and eastern North America are often associated with enhancement of the climatological tropospheric western ridge/eastern trough jet-stream pattern across the continent that can be instigated and maintained by SPV displacements. A significant shift of the SPV away from the central Arctic is evident as an elongated pattern, with a negative geopotential height center in the vicinity of Greenland (clusters 2 and 4 in figure 2). A connection may also exist between higher geopotential heights north of

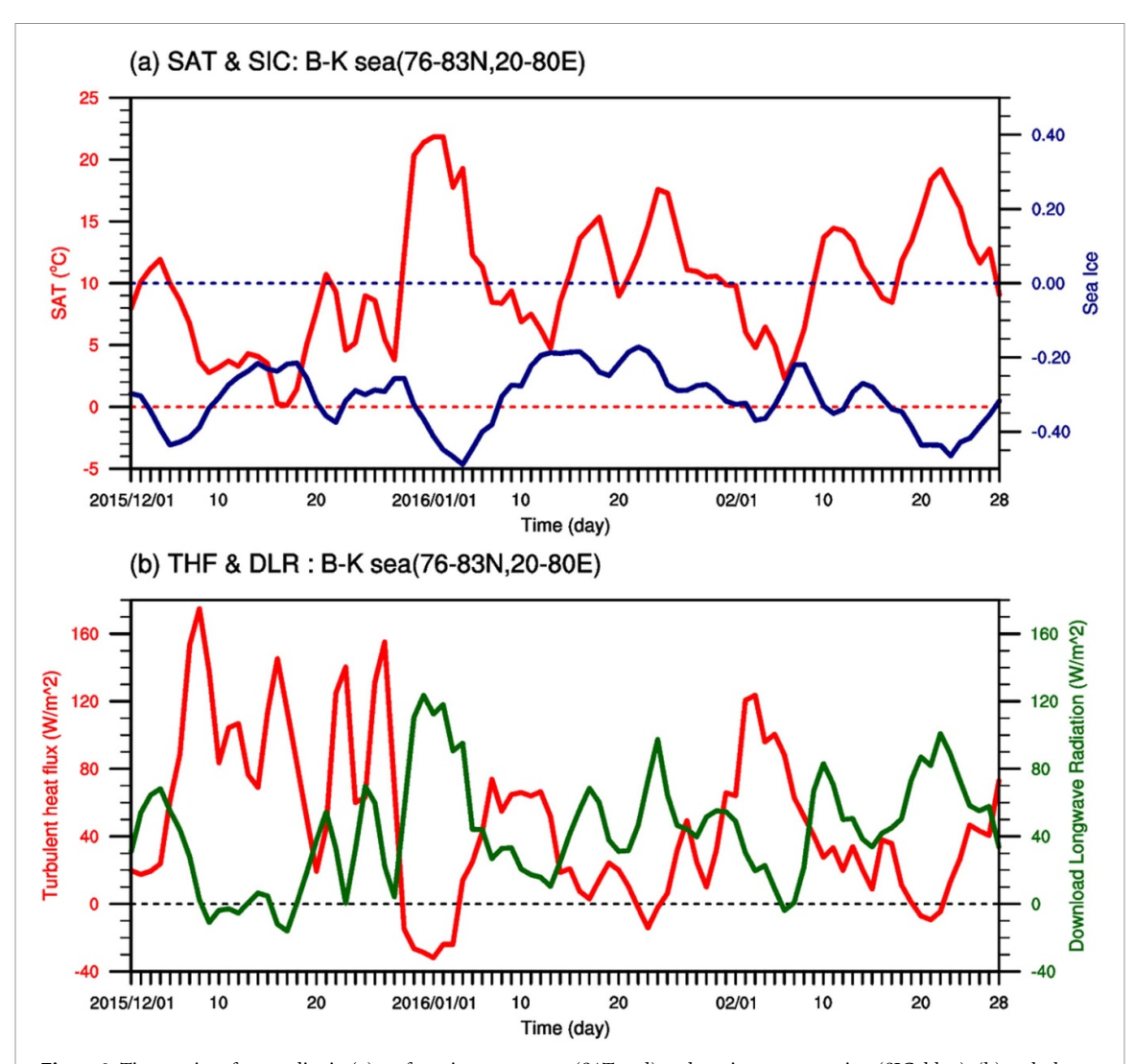


**Figure 8.** Time-series of anomalies in (a) surface air temperature (SAT; red) and sea-ice concentration (SIC; blue); (b) turbulent heat flux (THF; red) and downward longwave radiation (DLR; green) from 20 December 2015 to 10 February 2016 over BK Seas (76–83° N, 20–80° E). Note that positive (negative) DLR (THF) is directed downward. The analysis is based on the variables downloaded from Japan Meteorological Agency JRA-55 reanalysis (www.jra.kishou.go.jp/JRA-55/).

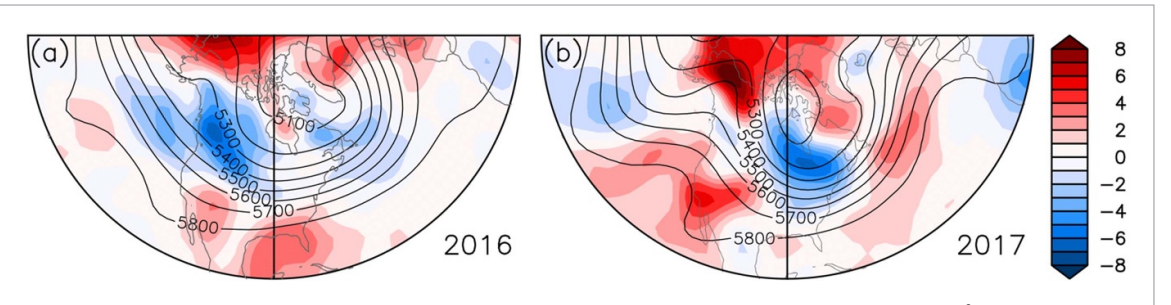


**Figure 9.** Mean 500 hPa geopotential heights (contours in m) and 925 hPa temperature anomalies (shading in  $^{\circ}$ C) for (a) 3–28 December 2016 and (b) 8–31 December 2017. The jet stream approximately follows the strongest gradient in the height contours. In 2017 positive temperature anomalies align well with the ridge in Alaska, and cold anomalies are located under the trough in eastern North America. Data from NCEP/NCAR reanalysis.

East Asia and lower heights over Greenland involving tropospheric/stratospheric coupling [52, 107, 108]. During February 2015 and 2018, for example, a positive temperature anomaly occurred in Alaska, while cold conditions persisted in eastern or central North America (figures 12(a) and (c)). Negative geopotential height anomalies at 500 hPa and 100 hPa were

nearly vertically collocated (figures 12(b) and (d)) [109]. During the winter of 2018 associated with this SPV disruption, record persistence of anomalous open water in the Bering and Chukchi Seas—and the resulting ocean-to-atmosphere heat transfer—helped to anchor and amplify a ridge in the polar jet stream, with a strong southerly flow aloft bringing unusually

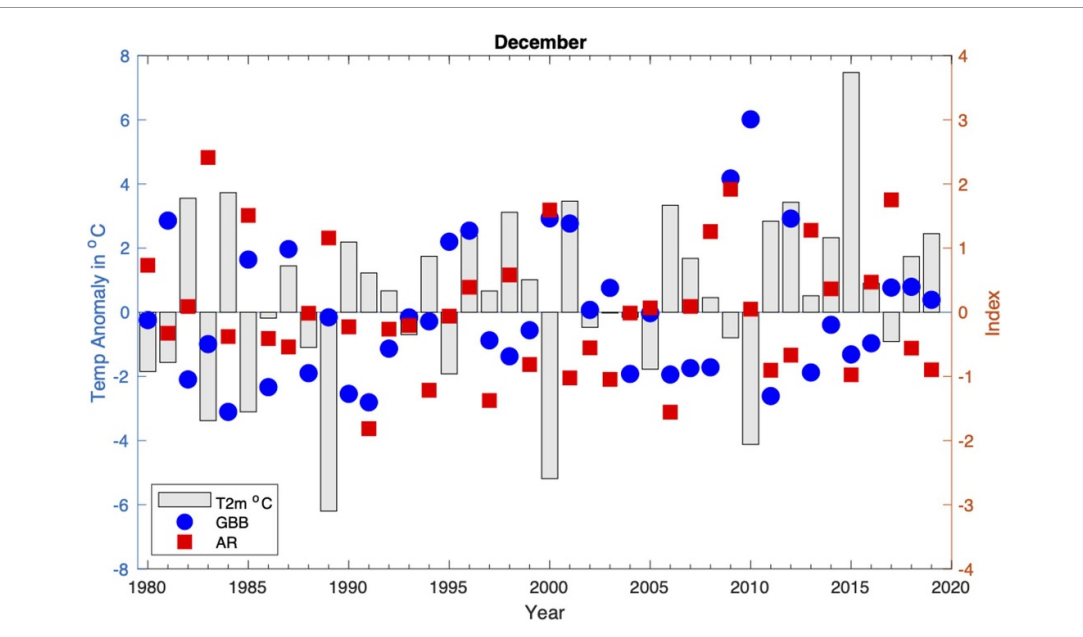


**Figure 10.** Time series of surface air temperature anomalies (T2m, grey bars) averaged over eastern U.S., indices of Greenland-Baffin Blocking (GBB, blue circles), and Alaska ridging (AR, red squares) for the month of December. GBB and AR are defined as the areal-averaged geopotential height anomaly at 700 hPa over domains: GBB: 60–75° N, 70–50° W; AR: 60–75° N, 150–130° W; NE America: 36–46° N, and 85–70° W. Data are based on NCEP/NCAR reanalysis, obtained from https://psl.noaa.gov/data/gridded/data.ncep.reanalysis.surface.html.

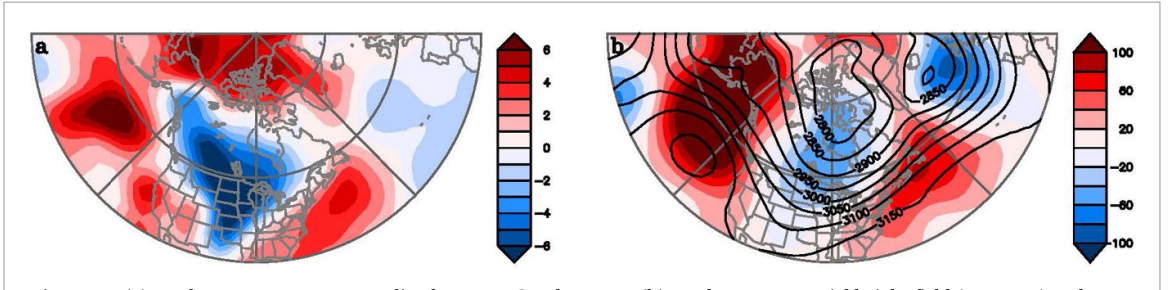


Figure 11. (a) 925 hPa temperature anomalies for 16–31 October 2020. (b) 700 hPa geopotential height field (contours) and anomalies (color shading; both in m). Data are from NCEP/NCAR reanalysis.

warm conditions to those regions [103]. Downstream (east) of this ridge, a deep trough persisted over Hudson Bay and western Canada, causing a prolonged and intense late-winter cold spell across central North America [110]. This pattern occurred again in January/February 2019, though in 2019 the pattern was shifted even farther westward relative to 2018. In 2015 (figures 12(a) and (b)) the trough was displaced east, resulting in anomalously cold temperatures across eastern North America.

Evidence suggests that late winters (JFM) during the AA era (since ~1990) featured more frequent amplified tropospheric ridge-trough longwave circulation patterns over North America [41, 110]. Extreme cold events (<-1.0 standard deviation) in eastern North America corresponding to an enhanced western ridge/eastern trough jet-stream pattern occurred during Februarys of 1959, 1967, 1976, 1989, 1990, 1992, 1995, 1997, 2000, 2002, 2011, 2014, 2015, 2018, and 2019 [108, 110, 111]. When this pattern sets up, persistent cold spells and heavy

snow events typically affect eastern North America, including the densely populated I-95 corridor from Boston to New York City and as far south as Washington, D.C [112]. Existence of an enhanced west-coast ridge also intensifies drought conditions in California [105]. When an amplified ridge/trough pattern exists over North America, the eastward propagation of the longwave jet-stream pattern tends to stagnate, thereby slowing the migration of weather systems across the continent and creating persistent weather conditions. Some studies [36, 39, 51] argue that the pattern is favored when low sea ice in the CB region occurs in combination with anomalously warm SSTs in the eastern North Pacific, as has been the case during most years since the Pacific Decadal Oscillation (PDO) shifted to its positive phase in winter 2013/14 [113–115].

It is unclear whether the intensification of the Alaskan ridge during late winter precedes or succeeds the downstream deepening of the aforementioned trough. These two circulation systems have been

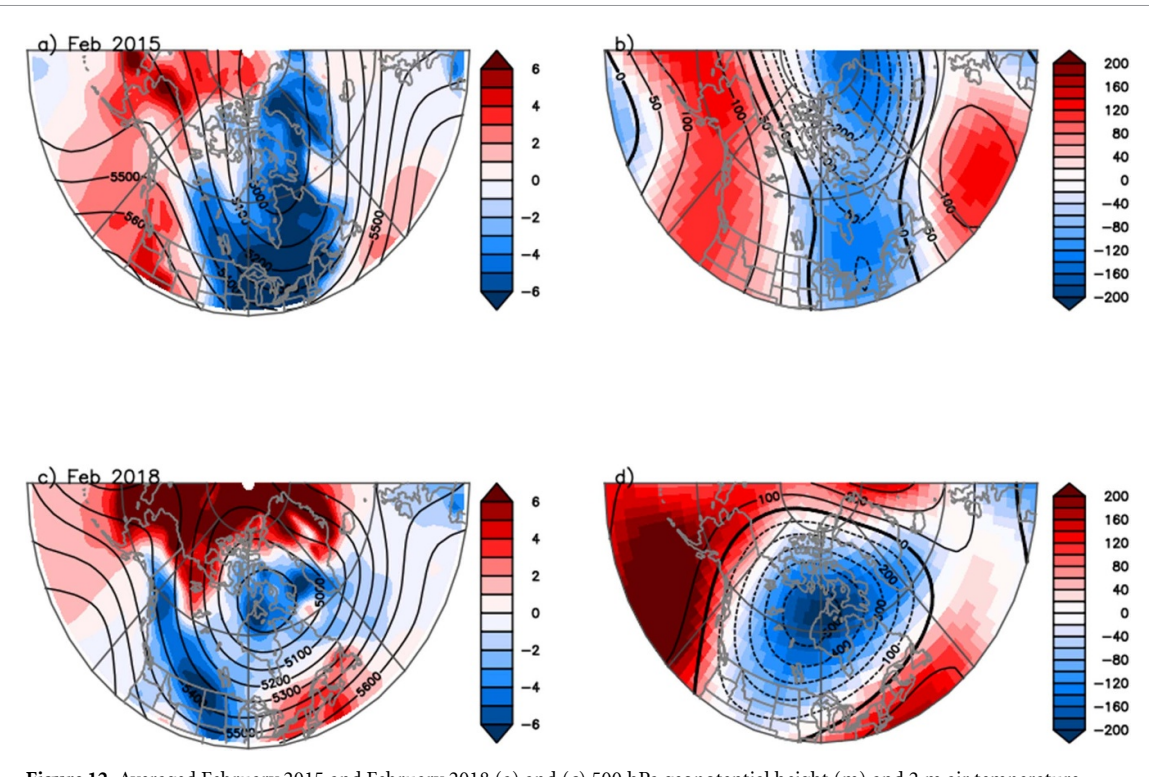
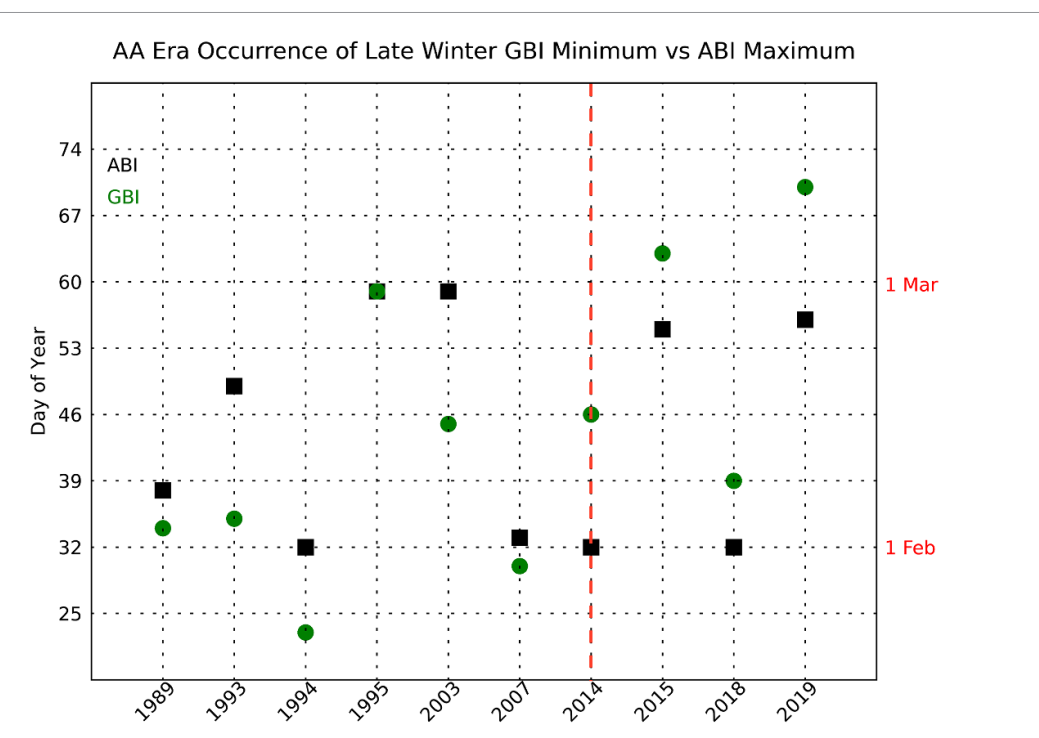


Figure 12. Averaged February 2015 and February 2018 (a) and (c) 500 hPa geopotential height (m) and 2 m air temperature anomalies (°C, shading), and (b) and (d) geopotential height anomalies (m) at 500 hPa (shading) and 100 hPa (contour). Data are from the NCEP/NCAR reanalysis.

hypothesized to act in concert to amplify an existing wavy jet pattern in recent decades [39, 51, 116]. Here we focus on the within-season timing of ridging in the vicinity of Alaska versus Greenland from 1989 through 2019. The frequency of both of these features has increased during this period (figure 13), but the temporal behavior is dominated by interannual variability. A metric defined as the Alaska Blocking Index (ABI) [117] describes the mean 500 hPa geopotential height field across greater Alaska: 54-76° N and 125-180° W; note the ABI (late winter) has a slightly different domain than AR (December) from earlier discussion (figure 10). The maximum daily ABI value within each month is compared with the lowest Greenland blocking index (GBI) value within  $\pm 14$  d of that anomaly (figure 12); note that the GBI's center is slightly east of the GBB used in figure 10. The Greenland trough (negative GBI) developed roughly one week before the Alaskan ridge for cases highlighted from 1989 to 2007, with the exception of concurrent ridge-trough extremes during late February of 1995. Since 2014, however, the Pacific ridge (i.e. ABI maximum) has strengthened [117] and has consistently preceded the formation of the Greenland trough by  $\sim 10$  d (figure 13). This change in behavior coincides with the shift in the PDO from its negative to positive phase [113], with anomalously warm SSTs in the northeastern North Pacific that favors development of a ridge in this location [36, 39]. This

suggests that NE Pacific SST anomalies are helping to drive the start of current jet stream sequencing, with the strengthening of the ABI due to constructive interference between the ridge and AA in the Pacific sector of the Arctic.

The timeseries analyses above (figures 10 and 13) [51], SPV disruptions, stratospheric congruence with tropospheric events (figure 12 [109]), recent anomalously warm SSTs in the northeast Pacific, and continued record low CB SICs during winter combine to support the hypothesis that background, pre-existing state-dependence of the longwave geopotential height pattern combined with warm air advection (Term B in equation (1)), are all factors helping to drive Arctic/midlatitude linkages that lead to extreme winter weather events over North America [35]. There has always been a connection among the jet stream, SPV, and U.S. cold spells (figures 10 and 13), and we argue that the connection may been further modulated by AA in certain wavy jet stream configurations. Other possible factors include time-lagged interactions involving thinner sea ice in winter, anomalous land-surface cooling rates, and Eurasian fall snow coverage; these phenomena create linkage mechanisms that involve anomalous surface/atmosphere turbulent heat fluxes, transient eddy activity, eddymean flow interactions, and vertical wave activity fluxes that can trigger or amplify SPV disruptions [36, 84, 118, 119].



**Figure 13.** Daily occurrence of the February/March Alaska Blocking Index (ABI) maximum (i.e. ridge) and Greenland blocking index (GBI) minimum (i.e. trough) since 1989. Years of anomalous monthly ABI values ( $>0.5\sigma$ ) are listed (1989, 1993, 1994, 1995, 2003, 2007, 2014, 2015, 2018, 2019) and the daily GBI minimum (green circles) are shown with respect to  $\pm 14$  d of the ABI maximum (black squares) within those years. Red dashed line indicates the switch from negative to positive Pacific Decadal Oscillation (PDO) in winter 2013/14. The ABI maximum and GBI minimum overlap in 1995. Data are from ERA-Interim Reanalysis.

### 4. European weather extremes

Extreme European winter weather is often related to the weakening of the SPV, seen as cluster 5 of figure 2. Table 2 lists recent anomalously cold winter months for Central England temperature (CET [120]) representing northwest Europe, defined by anomalies of at least 1.0 °C below the respective monthly mean for 1981–2010. The Table highlights the year-to-year intermittency of such events. The positive anomalies of the average 100 hPa polar cap geopotential height field anomaly (PCA) north of 60° N is an indicator of weakening of the SPV (table 2 right, figure 2 right), as is the proxy indicator, the negative AO. Winters in the United Kingdom during 2013/14, 2015/16, and 2019/20 were exceptionally mild, wet, and stormy, while winters during 2009/10 and 2010/11 were unusually cold with record snowfalls [121]; March 2013 was the coldest March in England since 1962. In late-winter 2018, extremely cold air invaded Europe from Siberia in an event known as the 'Beast from the East' following a SSW and disrupted SPV, giving the coldest March day in over a century over much of England and Wales [122, 123]. These events correspond with observed increases in interannual variability in the AO, NAO, jet latitude, and Greenland Blocking during winter [124, 125]. Synchrony exists among various largescale indices for some of these events, such as the AO/NAO and the GBI; a southward-shifted North

Atlantic polar jet stream (negative AO/NAO) generally coincided with high geopotential heights over Greenland, indicated by a positive GBI [126, 127].

These cases illustrate that different and sometimes multiple factors are associated with extreme cold spells in Europe. In March 2013, for example, extensive cold SATs persisted across northern Eurasia coincident with the SPV displaced to northern Siberia (figure 14). The evolution of the earlier events in table 2 (December-February 2009/10 and November-December 2010) contrasts with March 2013. During January/February 2010, blocking began over the Barents Sea, moved southward, then combined with a block that had developed in the western North Atlantic before shifting north over Greenland, and finally moving west toward Canada. During Nov/Dec 2010, which featured a record high December GBI value since the record began in 1850 and the coldest December CET value since 1890, a positive 500 hPa geopotential height anomaly formed over Scandinavia then moved west to form an intense Greenland block.

For the Beast-from-the-East case, in late February 2018 the SPV was displaced over northeast Canada similar to the pattern resolved by cluster 2 in figure 2 along with anomalously high stratospheric geopotential heights over Europe and associated tropospheric high pressure settling over Scandinavia and the Barents Sea. During March 2018 in contrast, observed 100 hPa geopotential heights featured a strong SPV

**Table 2.** North Atlantic/Arctic atmospheric circulation indices, Arctic Oscillation (AO), North Atlantic Oscillation (NAO), and Greenland blocking index (GBI), for recent anomalously cold winter months between winters (NDJFM) 2010 and 2020 inclusive in northwest Europe (defined by Central England Temperature (CET [120],) anomalies of at least 1.0 °C below the respective monthly mean for 1981–2010). AO is from the CPC website . NAO is from NCAR Climate data guide, and average polar cap height anomaly (PCA) north of 60° N is from NCAR/NCEP reanalysis.

Year	Month	CET anom.	AO	NAO	GBI	PCA
2009	December	-1.5	-3.41	-3.01	2.39	1.50
2010	January	-3.0	-2.59	-2.13	1.59	0.79
2010	February	-1.6	-4.27	-3.99	2.41	3.10
2010	November	-1.9	-0.38	-1.61	1.92	0.10
2010	December	-5.3	-2.63	-3.61	3.15	0.73
2013	February	-1.2	-1.01	-1.00	0.79	1.82
2013	March	-3.9	-3.18	-4.12	2.37	0.46
2016	November	-1.5	-0.61	-0.09	0.74	1.48
2018	February	-1.5	0.11	0.52	-1.06	1.34
2018	March	-1.7	-0.94	-2.29	1.33	0.88

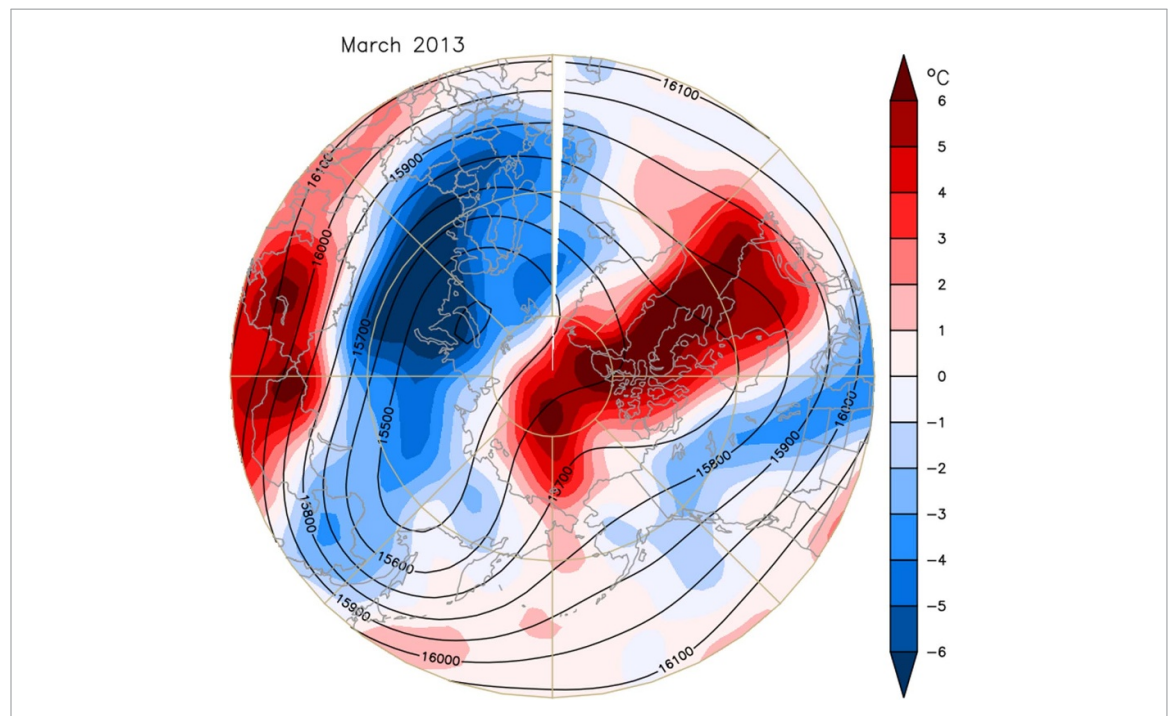


**Figure 14.** Air temperature anomalies at 925 hPa (°C, shading) and 100 hPa geopotential heights (m, contours) for March 2013. Data are from the NCEP/NCAR reanalysis.

center that shifted to Arctic Eurasia, also evident at 500 hPa. The time sequence of the late winter Beast-from-the-East case illustrates that internal variability of the SPV, and remote drivers including midand high-latitude blocking [123], were responsible for different forcing of the severe cold spells over Europe during February and March 2018.

Taken together, these four European examples (early and late 2010, March 2013, and February/-March 2018) indicate the sometimes importance of Greenland for reinforcing blocking, but blocking can initially develop elsewhere, typically either in the Norwegian or Siberian Arctic. High-latitude Greenland and SCAN blocks tend to be associated with an anomalous meridional circulation in the polar jet stream, thus providing an important conduit for poleward temperature and moisture advection and high to

midlatitude weather linkages [1, 126, 128]. In summary, European winter cold air outbreaks are often related to the weakening of the SPV and SSW [129]. In contrast to figure 2 that implies stationarity of SPV patterns, these studies show the importance of the movement of the SPV location, and forming daughter vortices in the case of splitting, within a winter season.

# 5. Potential tropical modulation of Arctic-midlatitude linkages

The SSW event in February 2018 has also been studied in conjunction with circulation and temperature anomalies arising from the Madden–Julian oscillation (MJO), the quasi-biennial oscillation (QBO), and El Niño-Southern Oscillation (ENSO). We briefly describe the MJO, QBO and ENSO and discuss their

possible roles in the context of the Arctic-midlatitude linkage.

The MJO is the dominant mode of intra-seasonal variability in the tropical troposphere on timescales typically around 40–50 d [130]. It consists of eastward propagation of large-scale circulation cells and organized cloud complexes from the Indian Ocean to the Pacific Ocean. The phase of MJO is captured by the EOF-based multivariate MJO index [131], which has eight phases closely matching the geographical location of the MJO-related enhancement of convection. Two phases are relevant to our discussion; the MJO phases 2–3 and 5–6 correspond to conditions with high convection activity in the tropical Indian Ocean and the western Pacific, respectively.

The QBO is an oscillation of zonal winds in the equatorial stratosphere at about 2 year intervals (see [132] for a review). During its easterly (westerly) phase, the SPV in the Northern Hemisphere tends to be weaker (stronger), known as the Holton–Tan relation [133, 134]. Through modulating stability in the tropical tropopause layer, the easterly QBO phase is associated with enhanced convective activity in the warm pool region, which generates a Rossby wave train that propagates into the midlatitude troposphere [135, 136].

ENSO is an interannual oscillation of the oceanatmosphere coupled system over the tropical Pacific, occurring typically at 3–5 year intervals, with related climate anomalies in many parts of the globe [137, 138]. During its warm phase (El Niño), a strong convective region moves eastward from its climatological position in the tropical western Pacific with positive SST and negative SLP anomalies to the tropical central/eastern Pacific.

The MJO, QBO and ENSO have timescales longer than synoptic, making them potential sources of improved sub-seasonal to seasonal prediction [139]. A study of the MJO in the 2018 SSW event suggested the importance of the record-breaking strength of MJO phase 6, with the amplification of wavenumber-2 planetary wave and associated teleconnection to this SSW [140]. Evidence is presented for the MJO phase 3 and 6 being precursors of the NAO regimes [141–143]. Low sea ice coverage in the BK is linked with a weaker SPV through enhanced upward propagation of planetary-scale waves.

Not only the MJO but ENSO and QBO phases favored a weak SPV for the 2018 SSW event [144]. MJO amplitude is significantly larger in the easterly phase of QBO, presumably with stronger signals in the extra-tropics via teleconnection [145]. Even without a joint influence with the MJO, the QBO has control on SPV strength, e.g. [132]. A first concern is the stratospheric pathway and downward influence of the weak SPV on the lower troposphere. A second part addresses if and how sea-ice variability influences the SPV that is already under strong influence by the QBO. When a high-top atmospheric general

circulation model was used to investigate the influence of the QBO, a weakening of the SPV was a response to sea ice loss under the easterly phase of the QBO through strengthened upward propagation of planetary-scale wave [146].

We analyzed the polar cap height (PCH) anomaly, defined as the averaged geopotential height anomaly for the area northward 60° N at the 50 hPa level, as a measure of the SPV strength and its relation with the QBO phase and BK ice conditions. Figure 15 shows how the PCH varies under different QBO and sea ice conditions. There is an apparent shift towards negative values (stronger SPV) for the QBOwest (QBOW) compared with the QBO-east (QBOE) (figure 15(b)). A similar shift within the QBOW high/low (H/L) ice composites is seen but is not significant (figure 15(c)). There is no clear difference in PCH anomalies between the high and low ice composites within the QBOE.

To ascertain whether the above description indicates joint influence from the QBO and sea ice on the strength of the SPV, we invoke dynamical evidence. A recent study found that weak SPV events, including SSWs, have distinct characteristics in upward propagation of planetary-scale waves depending on the sea ice condition, i.e. increased wavenumber-1 and wavenumber-2 E-P flux components in high and low sea conditions, respectively [80]. The anomalous structure in the wavenumber space under low sea ice and weak SPV conditions is similar to that under the low sea ice condition only, e.g. [147]. This is interpreted as indicating a sea ice influence on the SPV is constructive with respect to QBOE.

ENSO and its connection to the extratropics has been studied in a tropospheric and stratospheric context [148, 149]. Both observational and modelling studies document that during El Niño (La Niña) events the SPV is weakened (strengthened) by enhanced (reduced) upward planetary-scale wave propagation [150–152]. However, this relation is not always clear owing to the short observational record and the relatively long and irregular intervals between ENSO events [153, 154]. The tropospheric pathway is more active during El Niño, while the stratospheric pathway is more active during La Niña [155].

Tropical variability, such as the MJO, QBO, ENSO, and stratospheric/tropospheric vertical propagation, can influence Arctic sea ice, the NAO, and SPV, and modify sub-seasonal weather.

#### 6. Summary

In this review we discuss four aspects of Arctic/midlatitude connections that have so far received relatively little attention: (a) the differences between earlyand late-winter processes, (b) details of factors that can amplify synoptic cold events in Asia, North America, and Europe, (c) the role of SPV disruptions,

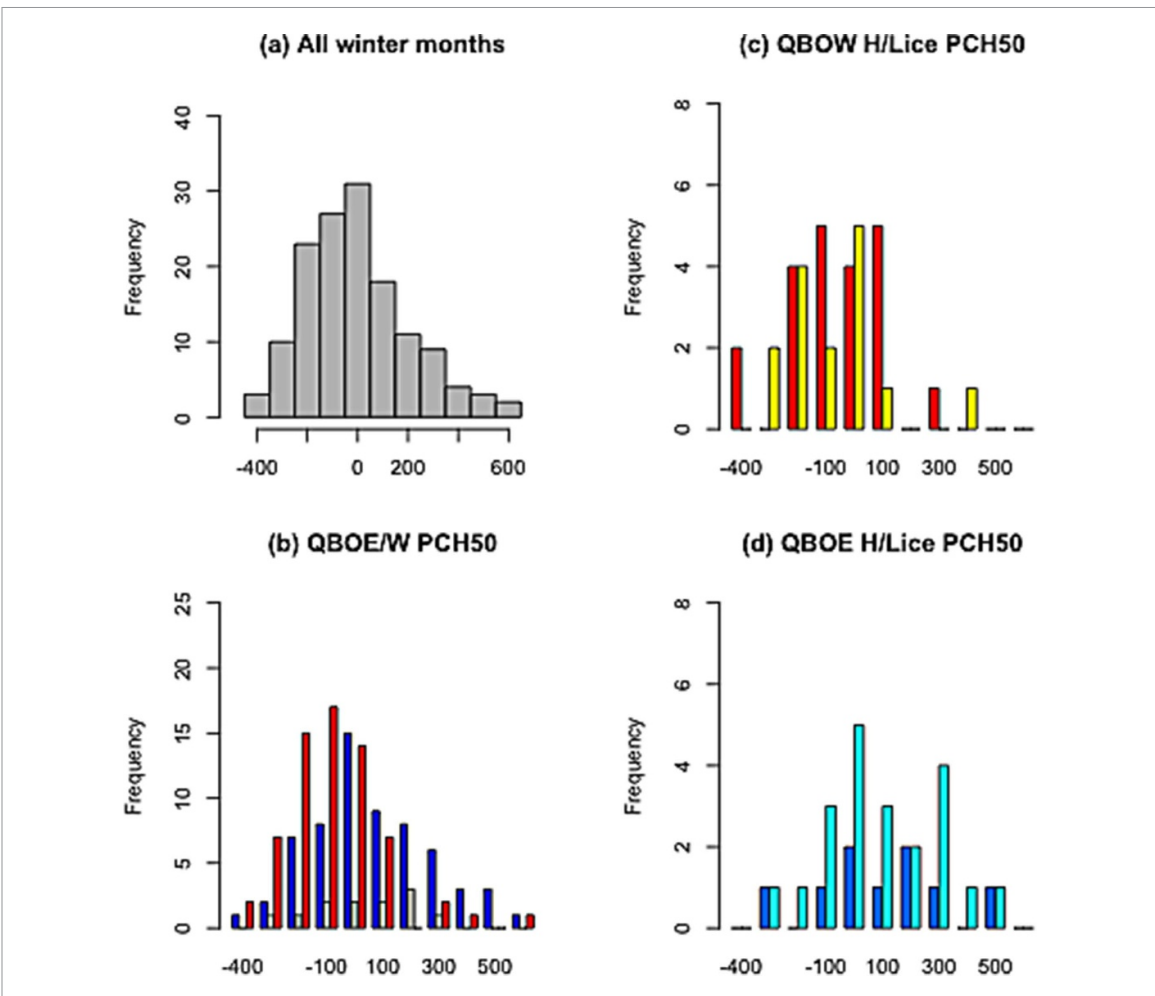


Figure 15. Frequency distributions of monthly mean polar cap height (PCH) anomalies (m) at 50 hPa for 1972/73- 2018/19 winter (DJF) months for (a) all winter months; (b) QBOW (red) and QBOE (blue) composites; (c) high-ice (red) and low-ice (yellow) groups within the QBOW composite; (d) high-ice (blue) and low-ice (light blue) groups within the QBOE composite. The QBOW and QBOE were defined using the criterion of  $\pm 3$  m s<sup>-1</sup> applied to the tropical (5° S-5° N mean) zonal-mean zonal wind at the 40 hPa level. For the sea ice condition, daily BK SIC anomalies were used after applying the second-order polynomial fitting and averaged for December with the  $\pm 0.5$  sigma criterion. Data are from the JRA-55 reanalysis and the HadISST2 sea ice data that includes the compilation of the National Ice Center sea ice chart.

and (d) tropical modulation of Arctic/midlatitude linkages.

Early winter Arctic/midlatitude weather linkages are more likely to involve reinforcement of teleconnection patterns for Eurasia and climatological jet-stream patterns for North America by surface enhancement related to delayed fall sea-ice freezeup primarily in the BK, CB, and BB, where early winter sea-ice reduction has been substantial. Upward surface energy flux over newly ice-free areas and poleward temperature advection (Terms C and B in equation (1)) increase the geopotential thickness and thus augment regional AA. Warm anomalies and positive geopotential height anomalies in both BK and CB initiate changes in existing large-scale atmospheric dynamics (Term A in equation (1)). During the early winter in Eurasia, an increase in the frequency of SCAN/Ural blocking is observed (figure 5) in association with the loss of BK sea ice [68, 128] and serves as a downstream forcing of individual synoptic weather events in East Asia, as well as a more frequent potential progenitor of Greenland blocking. The role of direct forcing from recent sea-ice-free areas appears secondary in this process relative to internal atmospheric variability, as modeling experiments forced by sea-ice variability alone produce weak atmospheric responses; but these experiments have been shown to understate AA and the corresponding responses (e.g. [12, 33],). Empirical and model evidence suggests that decreasing CB sea ice can strengthen ridging in the northeastern Pacific under the right atmospheric background conditions, thereby increasing persistence of the downstream trough and cold spells over central or eastern North America [51]. Constructive interaction between jetstream ridging along North America's west coast and regional heating is more likely when northeastern Pacific SSTs are anomalously warm, as was the case when the PDO phase shifted to a predominantly positive phase in 2014. Varying positions of the trough axis along with overall global warming reduces the likelihood of breaking cold records; both of these

factors contribute to the infrequent occurrence of extreme cold periods displayed in figure 10. The ridge location is critical for precipitation patterns along the west coast of North America, with extreme dry (wet) winters favored when the ridge is farther east (west).

Late-winter connections are less likely to involve surface fluxes related to sea-ice loss and open water. Instead, linkages occur in response to the formation of atmospheric blocks associated with disruptions and movement of the SPV [110], which are occasionally triggered by vertical propagation of wave energy from various sources at the surface or in the troposphere. An increasing trend in SPV disruptions/movements have been emerging in the mid-to-late winter, perhaps a consequence of AA in the peripheral Arctic seas.

In early winter the mean flow is inhibited at the Atlantic jet stream entrance region and atmospheric heat and moisture is meridionally advected into the Arctic (Term B in equation (1)). In late winter there is stronger zonal flow with a negative phase of the AO [155, 156]. Possible tropical modulation of Arctic/midlatitude linkages is from a constructive effect of the QBO and sea ice decline on the variability of PCH and SPV.

Attributing any particular extreme event or series of related events to one or more of the many factors that can excite them, including natural variability, remains challenging. In any given year, a different combination of factors and timing are in play with differing levels of influence, magnitudes of response, and locations of extremes. Causal relationships cannot be established purely through analysis of observed trends or covariability, while at present studies based on numerical models appear to be fall short in fully capturing the multiple interacting factors that cause extreme weather events [5, 34, 156, 157] nor a realistic strength of response [32, 33]. Modeling results should be challenged when observed values are an outlier relative to ensemble model means and to the probability distribution function of all individual members [53].

Simple cause-and-effect relationships between low sea ice, SPV variability, and subarctic and midlatitude tropospheric circulation anomalies are not consistent from event to event or from one year or season to the next [15]. An emerging insight is that regional Arctic and subarctic temperature anomalies may amplify (constructive interaction) or dampen (destructive interaction) a naturally occurring jetstream pattern rather than cause a particular event. Alternative physical explanations, such as internal atmospheric vorticity dynamics (figure 7), influence the initiation and/or persistence of blocking near Alaska, Greenland, and BK, which may then be modulated by changes in SST patterns, disruptions in the SPV, or tropical variability.

Further understanding of subarctic linkages would aid in predicting extreme weather events and

help society better prepare for future winters, as anthropogenic greenhouse gas concentrations continue to rise. The fact remains that the Arctic is an influential component of the global climate system, and it is challenging to conceive how three-quarters of its late-summer sea-ice volume can be lost over three decades with no implications for the Northern Hemisphere large-scale atmospheric circulation. Overall, the processes linking sea-ice variability, tropospheric teleconnection patterns, SST fluctuations, the SPV, and midlatitude severe winter weather remain a topic of great societal importance and active research, requiring the use of multiple datasets, metrics, models and methods to disentangle underlying mechanisms.

# Data availability statement

The data that support the findings of this study are openly available at the following URL/DOI: https://psl.noaa.gov/.

### Acknowledgments

- PMEL contribution 5081.
- Data are available from standard reanalysis and NSIDC products as noted in Figure captions: NCEP Reanalysis data provided by the NOAA/OAR/PSL, Boulder, Colorado, USA, from their Web site at https://psl.noaa.gov/. JRA55 Reanalysis data from Japanese Meteorological Agency (JMA), Tokyo, Japan downloaded from the following link: https://jra.kishou.go.jp/JRA-55/index\_en.html#download. HadISST data are available at following URL: www.metoffice.gov.uk/ hadobs/hadisst/data/download.html.
- We thank the anonymous reviewers for constructive suggestions that improved this manuscript.
- We thank M Kretschmer for important discussions on the vortex climatology.
- JEO and MW are supported by the NOAA Arctic Research Program. J Cohen is supported by the US National Science Foundation grants AGS-1657748 and PLR-1901352. TJB is supported by the University of Alaska Fairbanks Experimental Arctic Prediction Initiative. SJK is supported by the project (PE21010) of KOPRI. BMK is supported by the project 'Korea-Arctic Ocean Observing System (K-AOOS), KOPRI, 20160245)', funded by the MOF, Korea. JAF is supported by the Woodwell Climate Research Center, Falmouth MA. XZ is supported by the U.S. Department of Energy grant DE-SC0020640. EH was supported by IASC. TV was supported by the Academy of Finland (contract 317999). RJ is supported by the Helmholtz Climate Initiative REKLIM and the project SynopSys funded by the German Federal Ministry for Education and Research (Grant/Award

Number: 03F0872A). JU is supported by ArC-S/ArCSII and the Belmont Forum InterDec projects. This publication is partially funded by the Joint Institute for the Study of the Atmosphere and Ocean (JISAO) under NOAA Cooperative Agreement NA15OAR4320063, Contribution No 2020-1119.

- We appreciate the editorial support of Sandra Bigley at NOAA/PMEL.
- There are no conflicts of interest for any author.

#### **ORCID** iDs

J E Overland https://orcid.org/0000-0002-2012-8832

T J Ballinger https://orcid.org/0000-0002-8722-1927

J Cohen https://orcid.org/0000-0002-7762-4482 J A Francis https://orcid.org/0000-0002-7358-9296

R Jaiser https://orcid.org/0000-0002-5685-9637 B -M Kim https://orcid.org/0000-0002-1717-183X

S -J Kim https://orcid.org/0000-0002-6232-8082

T Vihma https://orcid.org/0000-0002-6557-7084

M Wang **b** https://orcid.org/0000-0001-5233-4588

X Zhang https://orcid.org/0000-0001-5893-2888

# References

- [1] Overland J E, Francis J, Hall R, Hanna E, Kim S-J and Vihma T 2015 The melting Arctic and midlatitude weather patterns: are they connected? J. Clim. 28 7917–32
- [2] Barnes E A and Screen J A 2015 The impact of Arctic warming on the midlatitude jet-stream: can it? Has it? Will it? WIRES Clim. Change 6 277–86
- [3] Francis J A 2017 Why are Arctic linkages to extreme weather still up in the air? *Bull. Am. Meteorol. Soc.* 98 2551–7
- [4] Blackport R and Screen J A 2020 Insignificant effect of Arctic amplification on the amplitude of mid-latitude atmospheric waves Sci. Adv. 6 eaay2880
- [5] Cohen J et al 2020 Divergent consensuses on Arctic amplification influence on midlatitude severe winter weather Nat. Clim. Change 10 20–29
- [6] Dai A and Song M 2020 Little influence of Arctic amplification on mid-latitude climate *Nat. Clim. Change* 10 231–7
- [7] Jung T et al 2016 Advancing polar prediction capabilities on daily to seasonal time scales *Bull. Am. Meteorol. Soc.* 97 1631–47
- [8] Rahmstorf S and Coumou D 2011 Increase of extreme events in a warming world *Proc. Natl Acad. Sci.* 108 17905–9
- [9] Richter-Menge J, Druckenmiller M L and Jeffries M (eds) 2019 Arctic Report Card 2019 (available at: www.arctic. noaa.gov/Report-Card)
- [10] Pörtner H-O et al (eds) (IPCC) 2019 IPCC Special Report on the Ocean and Cryosphere in a Changing Climate (available at: https://www.ipcc.ch/srocc/chapter/ technical-summary/)
- [11] Cohen J et al 2014 Recent Arctic amplification and extreme mid-latitude weather Nat. Geosci. 7 627–37

- [12] He S, Xu X, Furevik T and Gao Y 2020 Eurasian cooling linked to the vertical distribution of Arctic warming Geophys. Res. Lett. 47 e2020GL087212
- [13] Screen J A and Simmonds I 2013 Exploring links between Arctic amplification and mid-latitude weather *Geophys*. Res. Lett. 40 959–64
- [14] Barnes E A 2013 Revisiting the evidence linking Arctic amplification to extreme weather in midlatitudes *Geophys*. Res. Lett. 40 4734–9
- [15] Hassanzadeh P and Kuang Z 2015 Blocking variability: Arctic Amplification versus Arctic Oscillation Geophys. Res. Lett. 42 8586–95
- [16] Meleshko V P, Johannessen O M, Baidin A V, Pavlova T V and Govorkova V A 2016 Arctic amplification: does it impact the polar jet stream? *Tellus A* 68 32330
- [17] Shepherd T G 2016 Effects of a warming Arctic Science 353 989–90
- [18] Smith D M, Dunstone N J, Scaife A A, Fiedler E K, Copsey D and Hardiman S C 2017 Atmospheric response to Arctic and Antarctic sea ice: the importance of ocean-atmosphere coupling and the background state *J. Clim.* 30 4547–65
- [19] Kolstad E W and Screen J A 2019 Nonstationary relationship between autumn Arctic sea ice and the winter North Atlantic oscillation Geophys. Res. Lett. 46 7583–91
- [20] McGraw M C and Barnes E A 2020 New insights on subseasonal Arctic-midlatitude causal connections from a regularized regression model J. Clim. 33 213–28
- [21] Guan W, Jiang X, Ren X, Chen G and Ding Q 2020 Role of atmospheric variability in driving the 'warm-Arctic, cold-continent' pattern over the North America sector and sea ice variability over the Chukchi-Bering Sea *Geophys*. *Res. Lett.* 47 e2020GL088599
- [22] Blackport R, Screen J A, van der Wiel K and Bintanja R 2019 Minimal influence of reduced Arctic sea ice on coincident cold winters in mid-latitudes *Nat. Clim. Change* 9 697–704
- [23] Sato K, Inoue J and Watanabe M 2014 Influence of the Gulf Stream on the Barents Sea ice retreat and Eurasian coldness during early winter *Environ. Res. Lett.* 9 084009
- [24] McCusker K E, Fyfe J C and Sigmond M 2016 Twenty-five winters of unexpected Eurasian cooling unlikely due to Arctic sea ice loss *Nat. Geosci.* 9 838–42
- [25] Jin C, Wang B and Yang Y-M Y-M 2020 'Warm Arctic-cold Siberia' as an internal mode instigated by North Atlantic warming *Geophys. Res. Lett.* 47 e2019GL086248
- [26] Li M, Luo D, Simmonds I, Dai A, Zhong L and Yao Y 2020 Anchoring of atmospheric teleconnection patterns by Arctic Sea ice loss and its link to winter cold anomalies in East Asia Int. J. Climatol. 41 547–58
- [27] Screen J A 2017 The missing Northern European winter cooling response to Arctic sea ice loss *Nat. Commun.* 8 14603
- [28] Sorokina S A, Li C, Wettstein J and Kvamstø N 2016 Observed atmospheric coupling between Barents Sea ice and the warm-Arctic cold-Siberian anomaly pattern J. Clim. 29 495–511
- [29] Ding Q et al 2014 Tropical forcing of the recent rapid Arctic warming in northeastern Canada and Greenland Nature 509 209–12
- [30] Perlwitz J, Hoerling M and Dole R 2015 Arctic tropospheric warming: causes and linkages to lower latitudes J. Clim. 28 2154–67
- [31] Sigmond M and Fyfe J 2016 Tropical Pacific impacts on cooling North American winters Nat. Clim. Change 6 970–4
- [32] Mori M, Kosaka Y, Watanabe M, Nakamura H and Kimoto M 2019 A reconciled estimate of the influence of Arctic sea-ice loss on recent Eurasian cooling *Nat. Clim. Change* 9 123–9
- [33] Labe Z M, Peings Y and Magnusdottir G 2020 Warm Arctic, cold Siberia pattern: role of full Arctic amplification versus sea ice loss alone Geophys. Res. Lett. 47 e2020GL088583

- [34] Smith D M et al 2020 North Atlantic climate far more predictable than models imply Nature 583 796–800
- [35] Overland J E et al 2016 Nonlinear response of mid-latitude weather to the changing Arctic Nat. Clim. Change 6 992–9
- [36] Francis J A, Vavrus S J and Cohen J 2017 Amplified Arctic warming and mid-latitude weather: new perspectives on emerging connections WIREs Clim. Change 8 e474
- [37] Woollings T et al 2018 Daily to decadal modulation of jet variability J. Clim. 31 1297–314
- [38] Hall R J, Hanna E and Chen L 2021 Winter Arctic Amplification at the synoptic timescale, 1979–2018, its regional variation and response to tropical and extratropical variability Clim. Dyn. (https://doi.org/ 10.1007/s00382-020-05485-y)
- [39] Kug J-S, Jeong J-H, Jang Y-S, Kim B-M, Folland C K, Min S-K and Son S-W 2015 Two distinct influences of Arctic warming on cold winters over North America and East Asia Nat. Geosci. 8 759–62
- [40] Hanna E, Jones J, Cappelen J, Mernild S, Wood L and Steffen K 2013 The influence of North Atlantic atmospheric and oceanic forcing effects on 1900–2010 Greenland summer climate and ice melt/runoff *Int. J. Climatol.* 33 862–80
- [41] Francis J A and Vavrus S J 2015 Evidence for a wavier jet stream in response to rapid Arctic warming Environ. Res. Lett. 10 014005
- [42] Chen G, Lu J, Burrows D A and Leung L R 2015 Local finite-amplitude wave activity as an objective diagnostic of midlatitude extreme weather *Geophys. Res. Lett.* 42 10952–60
- [43] Cattiaux J, Peings Y, Saint-Martin D, Trou-Kechout N and Vavrus S J 2016 Sinuosity of midlatitude atmospheric flow in a warming world *Geophys. Res. Lett.* 43 8259–68 L070309
- [44] Röthlisberger M, Pfahl S and Martius O 2016 Regional-scale jet waviness modulates the occurrence of midlatitude weather extremes *Geophys. Res. Lett.* 43 10989–97
- [45] Vavrus S J, Wang F, Martin J E, Francis J A, Peings Y and Cattiaux J 2017 Changes in North American atmospheric circulation and extreme weather: influence of Arctic Amplification and Northern Hemisphere snow cover J. Clim. 30 4317–33
- [46] Hannachi A and Iqbal W 2019 On the nonlinearity of winter Northern Hemisphere atmospheric variability J. Atmos. Sci. 76 333–56
- [47] Screen J A and Simmonds I 2014 Amplified mid-latitude planetary waves favour particular regional weather extremes Nat. Clim. Change 4 704–9
- [48] Overland J E and Wang M 2015 Increased variability in early winter subarctic North American atmospheric circulation J. Clim. 28 7297–305
- [49] Holton J R 1979 An Introduction to Dynamic Meteorology (New York: Academic) 391 pp
- [50] Komatsu K K et al 2018 Poleward upgliding Siberian atmospheric rivers over sea ice heat up Arctic upper air Sci. Rep. 8 2872
- [51] Tachibana Y, Komatsu K K, Alexeev V A, Cai L and Ando Y 2019 Warm hole in Pacific Arctic sea ice cover forced mid-latitude Northern Hemisphere cooling during winter 2017–18 Sci. Rep. 9 5567
- [52] Kretschmer M, Cohen J, Matthias V, Runge J and Coumou D 2018 The different stratospheric influence on cold-extremes in Eurasia and North America npj Clim. Atmos. Sci. 1 44
- [53] Sun L, Perlwitz J and Hoerling M 2016 What caused the recent 'Warm Arctic, Cold Continents' trend pattern in winter temperatures? *Geophys. Res. Lett.* 43 5345–52
- [54] Woo S-H, Kim B-M, Jeong J-H, Kim S-J and Lim G-H 2012 Decadal changes in surface air temperature variability and cold surge characteristics over northeast Asia and their relation with the Arctic Oscillation for the past three decades (1979–2011) J. Geophys. Res. Atmos. 117 D18117

- [55] Tang Q, Zhang X, Yang X and Francis F 2013 Cold winter extremes in northern continents linked to Arctic sea ice loss *Environ. Res. Lett.* 8 014036
- [56] Wu B, Handorf D, Dethloff K, Rinke A and Hu A 2013 Winter weather patterns over Northern Eurasia and Arctic sea ice loss Mon. Weather Rev. 141 3786–800
- [57] Wu B, Yang K and Francis J A 2017 A cold event in Asia during January–February 2012 and its possible association with Arctic sea ice loss J. Clim. 30 7971–90
- [58] Kim B-M et al 2014 Weakening of the stratospheric polar vortex by Arctic sea ice loss Nat. Commun. 5 4646
- [59] Honda M, Inoue J and Yamane S 2009 Influence of low Arctic sea-ice minima on anomalously cold Eurasian winters Geophys. Res. Lett. 36 L08707
- [60] Mori M, Watanabe M, Shiogama H, Inoue J and Kimoto M 2014 Robust Arctic sea-ice influence on the frequent Eurasian cold winters in past decades *Nat. Geosci.* 7 869–73
- [61] Nakamura T, Yamazaki K, Iwamoto K, Honda M, Miyoshi Y, Ogawa Y and Ukita J 2015 A negative phase shift of the winter AO/NAO due to the recent Arctic sea-ice reduction in late autumn J. Geophys. Res. Atmos. 120 3209–27
- [62] Park H-S, Kim S-J, Seo K-H, Stewart A L, Kim S-Y and Son S-W 2018 The impacts of Arctic sea ice loss on mid-Holocene climate Nat. Commun. 9 4571
- [63] Sung M-K, Kim S-H, Kim B-M and Choi Y-S 2018 Interdecadal variability of the warm Arctic and cold Eurasia pattern and its North Atlantic origin J. Clim. 31 5793–810
- [64] Zhang X, Sorteberg A, Zhang J, Gerdes R and Comiso J C 2008 Recent radical shifts in atmospheric circulations and rapid changes in Arctic climate system *Geophys. Res. Lett.* 35 L22701
- [65] Tyrlis E, Manzini E, Bader J, Ukita J, Nakamura H and Matei D 2019 Ural blocking driving extreme Arctic sea ice loss, cold Eurasia, and stratospheric vortex weakening in autumn and early winter 2016–2017 J. Geophys. Res. Atmos. 124 11313–29
- [66] Vihma T 2014 Effects of Arctic sea ice decline on weather and climate: a review Surv. Geophys. 35 1175–214
- [67] Vavrus S J 2018 The influence of Arctic amplification on mid-latitude weather and climate Curr. Clim. Change Rep. 4 238–49
- [68] Crasemann B, Handorf D, Jaiser R, Dethloff K, Nakamura T, Ukita J and Yamazaki K 2017 Can preferred atmospheric circulation patterns over the North-Atlantic-Eurasian region be associated with Arctic sea ice loss? *Polar Sci.* 14 9–20
- [69] Day J J, Sandu I, Magnusson L, Rodwell M J, Lawrence H, Bormann N and Jung T 2019 Increased Arctic influence on the midlatitude flow during Scandinavian Blocking episodes Q. J. R. Meteorol. Soc. 145 3846–62
- [70] Peings Y 2019 Ural blocking as a driver of early-winter stratospheric warmings Geophys. Res. Lett. 46 5460–8
- [71] Bueh C and Nakamura H 2007 Scandinavian pattern and its climatic impact Q. J. R. Meteorol. Soc. 133 2117–31
- [72] Cheung H N, Zhou W, Shao Y, Chen W, Mok H and Wu M 2013 Observational climatology and characteristics of wintertime atmospheric blocking over Ural-Siberia Clim. Dyn. 41 63–79
- [73] Zhang X, Lu C and Guan Z 2012 Weakened cyclones, intensified anticyclones, and the recent extreme cold winter weather events in Eurasia Environ. Res. Lett. 7 044044
- [74] Takaya K and Nakamura H 2005 Mechanisms of intraseasonal amplification of the cold Siberian High J. Atmos. Sci. 62 4423–40
- [75] Kretschmer M, Coumou D, Donges J F and Runge J 2016 Using causal effect networks to analyze different Arctic drivers of midlatitude winter circulation *J. Clim.* 29 4069–81
- [76] Zhang P, Wu Y, Simpson I R, Smith K L, Zhang X, De B and Callaghan P 2018 A stratospheric pathway linking a

- colder Siberia to Barents-Kara Sea ice loss *Sci. Adv.* 4 eaat6025
- [77] Jaiser R, Dethloff K, Handorf D, Rinke A and Cohen J 2012 Impact of sea ice cover changes on the Northern Hemisphere atmospheric winter circulation *Tellus A* 64 11595
- [78] Jaiser R, Nakamura T, Handorf D, Dethloff K, Ukita J and Yamazaki K 2016 Atmospheric winter response to Arctic sea ice changes in reanalysis data and model simulations J. Geophys. Res. Atmos. 121 7564–77
- [79] Nakamura T, Yamazaki K, Honda M, Ukita J, Jaiser R, Handorf D and Dethloff K 2016 On the atmospheric response experiment to a Blue Arctic Ocean Geophys. Res. Lett. 43 10394–402
- [80] Hoshi K, Ukita J, Honda M, Nakamura T, Yamazaki K, Miyoshi Y and Jaiser R 2019 Weak stratospheric polar vortex events modulated by the Arctic sea ice loss J. Geophys. Res. Atmos. 124 858–69
- [81] Screen J A et al 2018 Consistency and discrepancy in the atmospheric response to Arctic sea ice loss across climate models Nat. Geosci. 11 153–63
- [82] Baldwin M P and Dunkerton T J 2001 Stratospheric harbingers of anomalous weather regimes Science 294 581–4
- [83] Butler A H, Sjoberg J P, Seidel D J and Rosenlof K H 2017 A sudden stratospheric warming compendium Earth Syst. Sci. Data 9 63–76
- [84] Cohen J, Barlow M, Kushner P and Saito K 2007 Stratosphere–troposphere coupling and links with Eurasian land-surface variability J. Clim. 20 5335–43
- [85] Gastineau G, L'Hévéder B, Codron F and Frankignoul C 2016 Mechanisms determining the winter atmospheric response to the Atlantic overturning circulation *J. Clim.* 29 3767–85
- [86] Orsolini Y, Senan R, Vitart F, Balsamo G, Weisheimer A and Doblas-Reyes F J 2016 Influence of the Eurasian snow on the negative North Atlantic Oscillation in subseasonal forecasts of the cold winter Clim. Dyn. 47 1325–34
- [87] Nakamura T, Yamazaki K, Sato T and Ukita J 2019 Memory effects of Eurasian land processes cause enhanced cooling in response to sea ice loss Nat. Commun. 10 5111
- [88] Lee S H and Butler A H 2020 The 2018–2019 Arctic stratospheric polar vortex Weather 75 52–57
- [89] Luo D, Xiao Y, Yao Y, Dai A, Simmonds I and Franzke C 2016 Impact of Ural blocking on winter warm Arctic—cold Eurasian anomalies. Part I: blocking-induced amplification I. Clim. 29 3925–47
- [90] Luo D, Chen X, Overland J, Simmonds I, Wu Y and Zhang P 2019 Weakened potential vorticity barrier linked to Arctic sea-ice loss and increased mid-latitude cold extremes J. Clim. 32 4235–61
- [91] Binder H, Boettcher M, Grams C M, Joos H, Pfahl S and Wernli H 2017 Exceptional air mass transport and dynamical drivers of an extreme wintertime Arctic warm event *Geophys. Res. Lett.* 44 12028–36.
- [92] Kim B-M et al 2017 Major cause of unprecedented Arctic warming in January 2016: critical role of an Atlantic windstorm Sci. Rep. 7 40051
- [93] Boisvert L N, Petty A and Stroeve J C 2016 The impact of the extreme winter 2015/16 Arctic cyclone on the Barents–Kara Seas Mon. Weather Rev. 144 4279–87
- [94] Cullather R I, Lim Y-K, Boisvert L N, Brucker L, Lee J N and Nowicki S M J 2016 Analysis of the warmest Arctic winter, 2015–2016 Geophys. Res. Lett. 43 10808–16
- [95] Moore G W K 2016 The December 2015 North Pole warming event and the increasing occurrence of such events Sci. Rep. 6 39084
- [96] Wang S-Y S, Lin Y-H, Lee M-Y, Yoon J-H, Meyer J D D and Rasch P J 2017 Accelerated increase in the Arctic tropospheric warming events surpassing stratospheric warming events during winter *Geophys. Res. Lett.* 44 3806–15

- [97] Luo D and Zhang W 2020 A nonlinear multiscale theory of atmospheric blocking: dynamical and thermodynamic effects of meridional potential vorticity gradient *J. Atmos.* Sci. 77 2471–500
- [98] Takaya K and Nakamura H 2005 Geographical dependence of upper-level blocking formation associated with intraseasonal amplification of the Siberian high *J. Atmos.* Sci. 62 4441–9
- [99] Zhou W, Chan J C L, Chen W, Ling J, Pinto J G and Shao Y 2009 Synoptic-scale controls of persistent low temperature and icy weather over southern China in January 2008 Mon. Weather Rev. 137 3978–91
- [100] Woods C and Caballero R 2016 The role of moist intrusions in winter Arctic warming and sea ice decline J. Clim. 29 4473–85
- [101] Lee S, Gong T, Feldstein S, Screen J and Simmonds I 2017 Revisiting the cause of the 1989–2009 Arctic surface warming using the surface energy budget: downward infrared radiation dominates the surface fluxes *Geophys*. *Res. Lett.* 44 10654–10,661
- [102] Zhong L, Hua L and Luo D 2018 Local and external moisture sources for the Arctic warming over the Barents–Kara Seas J. Clim. 31 1963–82
- [103] Overland J E and Wang M 2018 Arctic-midlatitude weather linkages in North America Polar Sci. 16 1–9
- [104] Kodaira T, Waseda T, Nose T and Inoue J 2020 Record high Pacific Arctic seawater temperatures and delayed sea ice advance in response to episodic atmospheric blocking Sci. Rep. 10 20830
- [105] Swain D L, Horton D E, Singh D and Diffenbaugh N S 2016 Trends in atmospheric patterns conducive to seasonal precipitation and temperature extremes in California Sci. Adv. 2 e1501344
- [106] Blackport R and Screen J A 2020 Weakened evidence for mid-latitude impacts of Arctic warming Nat. Clim. Change 10 1065–6
- [107] Kodera K, Mukougawa H, Maury P, Ueda M and Claud C 2016 Absorbing and reflecting sudden stratospheric warming events and their relationship with tropospheric circulation J. Geophys. Res. Atmos. 121 80–94
- [108] Lee S H, Furtado J C and Charlton-Perez A J 2019 Wintertime North American weather regimes and the Arctic stratospheric polar vortex *Geophys. Res. Lett.* 46 14892–900
- [109] Kidston J, Scaife A A, Hardiman S C, Mitchell D M, Butchart N, Baldwin M P and Gray L J 2015 Stratospheric influence on tropospheric jet streams, storm tracks and surface weather Nat. Geosci. 8 433–40
- [110] Overland J E and Wang M 2019 Impact of the winter polar vortex on greater North America Int. J. Climatol. 39 5815–21
- [111] Huang J, Ou T, Chen D, Luo Y and Zhao Z 2019 The amplified Arctic warming in the recent decades may have been overestimated by CMIP5 models *Geophys. Res. Lett.* 46 13338–45
- [112] Cohen J, Pfeiffer K and Francis J A 2018 Warm Arctic episodes linked with increased frequency of extreme winter weather in the United States Nat. Commun. 9 869
- [113] Screen J A and Francis J A 2016 Contribution of sea-ice loss to Arctic amplification is regulated by Pacific Ocean decadal variability Nat. Clim. Change 6 856–60
- [114] Sung M-K, Kim B-M, Baek E-H, Lim Y-K and Kim S-J 2016 Arctic-North Pacific coupled impacts on the late autumn cold in North America Environ. Res. Lett. 11 084016
- [115] Tao L, Sun X and Yang X-Q 2019 The asymmetric atmospheric response to the midlatitude North Pacific SST anomalies J. Geophys. Res. Atmos. 124 9222–40
- [116] Lee M-Y, Hong -C-C and Hsu -H-H 2015 Compounding effects of warm sea surface temperature and reduced sea ice on the extreme circulation over the extratropical North Pacific and North America during the 2013–2014 boreal winter *Geophys. Res. Lett.* 42 1612–8

- [117] McLeod J T, Ballinger T J and Mote T L 2018 Assessing the climatic and environmental impacts of mid-tropospheric anticyclones over Alaska Int. J. Climatol. 38 351–64
- [118] Basu S, Zhang X, Polyakov I and Bhatt U S 2013 North American winter-spring storms: modeling investigation on tropical Pacific sea surface temperature impacts *Geophys*. *Res. Lett.* 40 5228–33
- [119] Jaiser R, Dethloff K and Handorf D 2013 Stratospheric response to Arctic sea ice retreat and associated planetary wave propagation changes *Tellus* A 65 19375
- [120] Parker D, Legg T and Folland C 1992 A new daily Central England temperature series 1772–1991 Int. J. Clim. 12 317–42
- [121] Hanna E, Hall R J and Overland J E 2017 Can Arctic warming influence extreme UK weather? Weather 72 346–52
- [122] Greening K and Hodgson A 2019 Atmospheric analysis of the cold late February and early March 2018 over the UK Weather 74 79–85
- [123] Overland J E, Hall R J, Hanna E, Karpechko A, Vihma T, Wang M and Zhang X 2020 The polar vortex and extreme weather: the Beast from the East in winter 2018 Atmosphere 11 664
- [124] Hanna E, Cropper T E, Jones P D, Scaife A A and Allan R 2015 Recent seasonal asymmetric changes in the NAO (a marked summer decline and increased winter variability) and associated changes in the AO and Greenland Blocking Index Int. J. Climatol. 35 2540–54
- [125] Zhang W and Luo D 2020 A nonlinear theory of atmospheric blocking: an application to Greenland blocking changes linked to winter Arctic sea ice loss J. Atmos. Sci. 77 723–51
- [126] Hanna E, Cropper T E, Hall R J and Cappelen J 2016 Greenland blocking index 1851–2015: a regional climate change signal Int. J. Climatol. 36 4847–61
- [127] Charlton-Perez A J, Ferranti L and Lee R 2018 The influence of the stratospheric state on North Atlantic weather regimes Q. J. R. Meteorol. Soc. 144 1140–51
- [128] Vihma T et al 2020 Effects of the tropospheric large-scale circulation on European winter temperatures during the period of amplified Arctic warming Int. J. Climatol. 40 509–29
- [129] Zhang P, Wu Y, Chen G and Yu Y 2020 North American cold events following sudden stratospheric warming in the presence of low Barents–Kara Sea sea ice *Environ. Res. Lett.* 15 124017
- [130] Madden R A and Julian P R 1994 Observations of the 40–50-day tropical oscillation—a review Mon. Weather Rev. 122 814–37
- [131] Wheeler M C and Hendon H H 2004 An all-season real-time multivariate MJO index: development of an index for monitoring and prediction *Mon. Weather Rev.* 132 1917–32
- [132] Anstey J A and Shepherd T D 2014 High-latitude influence of the quasi-biennial oscillation Q. J. R. Meteorol. Soc. 140 1–21
- [133] Holton J R and Tan H C 1980 The influence of the equatorial quasi-biennial oscillation on the global circulation at 50 mb J. Atmos. Sci. 37 2200–8
- [134] Holton J R and Tan H C 1982 The quasi-biennial oscillation in the Northern Hemisphere lower stratosphere J. Meteorol. Soc. Japan 60 140–8
- [135] Gray W M, Sheaffer J D and Knaff J A 1992 Hypothesized mechanism for stratospheric QBO influence on ENSO variability *Geophys. Res. Lett.* 19 107–10
- [136] Yamazaki K, Nakamura T, Ukita J and Hoshi K 2020 A tropospheric pathway of the stratospheric quasi-biennial oscillation (QBO) impact on the boreal winter polar vortex Atmos. Chem. Phys. 20 5111–27
- [137] Trenberth K E, Caron J M, Stepaniak D P and Worley S 2002 Evolution of El Niño-Southern Oscillation and

- global atmospheric surface temperatures *J. Geophys. Res.* **107** 4065
- [138] Wallace J M, Rasmusson E M, Mitchell T P, Kousky V E, Sarachik E S and von Storch H 1998 On the structure and evolution of ENSO-related climate variability in the tropical Pacific: lessons from TOGA J. Geophys. Res. 103 14241–14259
- [139] Domeisen D I V et al 2020 The role of the stratosphere in subseasonal to seasonal prediction: 2. Predictability arising from stratosphere-troposphere coupling J. Geophys. Res. 125 e2019ID030923
- [140] Statnaia I A, Karpechko A Y and Jarvinen H J 2020 Mechanisms and predictability of sudden stratospheric warming in winter 2018 Weather Clim. Dyn. 1 657–74
- [141] Cassou C 2008 Intraseasonal interaction between the Madden-Julian Oscillation and the North Atlantic Oscillation Nature 455 523–7
- [142] Garfinkel C I, Feldstein S B, Waugh D W, Yoo C and Lee S 2012 Observed connection between stratospheric sudden warmings and the Madden-Julian Oscillation Geophys. Res. Lett. 39 I 18807
- [143] Ukita J, Honda M, Nakamura H, Tachibana Y, Cavalieri D J, Parkinson C L, Koide H and Yamamoto K 2007 Northern Hemisphere sea ice variability: lag structure and its implications *Tellus* A 59 261–72
- [144] Barrett B S 2019 Connections between the Madden–Julian Oscillation and surface temperatures in winter 2018 over eastern North America Atmos. Sci. Lett. 20 e869
- [145] Yoo C and Son S-W 2016 Modulation of the boreal wintertime Madden-Julian oscillation by the stratospheric quasi-biennial oscillation *Geophys. Res. Lett.* 43 1392–8
- [146] Labe Z, Peings Y and Magnusdottir G 2019 The effect of QBO phase on the atmospheric response to projected Arctic sea ice loss in early winter *Geophys. Res. Lett.* 46 7663–71
- [147] Hoshi K et al 2017 Poleward eddy heat flux anomalies associated with recent Arctic sea ice loss Geophys. Res. Lett. 44 446–54
- [148] Horel J D and Wallace J M 1981 Planetary scale atmospheric phenomena associated with the Southern Oscillation Mon. Weather Rev. 109 813–29
- [149] van Loon H and Labitzke K 1987 The Southern Oscillation. Part V: the anomalies in the lower stratosphere of the Northern Hemisphere in winter and a comparison with the quasi-biennial oscillation Mon. Weather Rev. 115 357–69
- [150] Brönnimann S 2007 Impact of El Niño-Southern Oscillation on European climate Rev. Geophys. 45 RG3003
- [151] Cagnazzo C and Manzini E 2009 Impact of the stratosphere on the winter tropospheric teleconnections between ENSO and the North Atlantic and European region *J. Clim.* 22 1223–38
- [152] Ineson S and Scaife A 2009 The role of the stratosphere in the European climate response to Niño Nat. Geosci. 2 32–36
- [153] Jiménez-Esteve B and Domeisen D I V 2020 Nonlinearity in the tropospheric pathway of ENSO to the North Atlantic Weather Clim. Dvn. 1 225–45
- [154] Domeisen D I V, Garfinkel C I and Butler A H 2018 The teleconnection of El Niño Southern Oscillation to the stratosphere Rev. Geophys. 57 5–47
- [155] Jaiser R, Handorf D and Dethloff K 2019 Interaction of diabatic processes, large-scale eddies and the mean atmospheric circulation over the Atlantic, Arctic and Eurasia Adv. Polar Sci. 30 81–92
- [156] Smith D M et al 2019 The Polar Amplification Model Intercomparison Project (PAMIP) contribution to CMIP6: investigating the causes and consequences of polar amplification Geosci. Model Dev. 12 1139–64
- [157] Lee R W, Woolnough S J, Charlton-Perez A J and Vitart F 2019 ENSO modulation of MJO teleconnections to the North Atlantic and Europe Geophys. Res. Lett. 46 13535–45